RSC Advances

REVIEW

View Article Online
View Journal | View Issue

Cite this: *RSC Adv.*, 2022, **12**, 23481

Recent developments in hydrogels containing copper and palladium for the catalytic reduction/degradation of organic pollutants

Jaber Dadashi, [a] Mohammad Ali Ghasemzadeh *[b] and Masoud Salavati-Niasari [c]

The elimination of toxic and hazardous contaminants from different environmental media has become a global challenge, causing researchers to focus on the treatment of pollutants. Accordingly, the elimination of inorganic and organic pollutants using sustainable, effective, and low-cost heterogeneous catalysts is considered as one of the most essential routes for this aim. Thus, many efforts have been devoted to the synthesis of novel compounds and improving their catalytic performance. Recently, palladium- and copper-based hydrogels have been used as catalysts for reduction, degradation, and decomposition reactions because they have significant features such as high mechanical strength, thermal stability, and high surface area. Herein, we summarize the progress achieved in this field, including the various methods for the synthesis of copper- and palladium-based hydrogel catalysts and their applications for environmental remediation. Moreover, palladium- and copper-based hydrogel catalysts, which have certain advantages, including high catalytic ability, reusability, easy work-up, and simple synthesis, are proposed as a new group of effective catalysts.

Received 1st June 2022
Accepted 27th July 2022

DOI: 10.1039/d2ra03418b

rsc.li/rsc-advances

1. Introduction

Environmental pollution induced by industrial development and increase in population affects the life of living organisms by increasing the production of dangerous and toxic compounds such as organic dyes and food waste. Thus, this global problem has received much attention from researchers.[1]

Among the various pollutants, oil spills, heavy metals, herbicides, organic compounds, fertilizers, and sewage are considered the most important.[2] Nitro compounds as one of the main pollutant groups are usually found in water. For instance, 4-nitrophenol, a key industrial pollutant, poses a threat to the ecosystem and human health when released into the environment owing to its high chemical stability and toxicity.[3–5] Organic dyes are another group of compounds that pollute the environment. Synthetic organic dyes, which are poisonous, bio refractory, and carcinogenic pollutants, have become a significant source of water contamination. Because these dyes are chemically and physiologically persistent in the environment, the typical degradation processes are unsuitable for their separation.[6–8] Furthermore, although there are various methods to remove pollutants from water and the environment, some of them are specific to certain uses. For example, coagulation, chemical reduction, reverse osmosis, and photodegradation procedures are used to remove nitro compounds and organic dyes.[9–11] Scheme 1 provides the different approaches for the elimination of pollutants including absorption, chemical reactions, adsorption, photocatalysis, and filtration.[12–23] Some of these methods are simple, inexpensive, with low energy consumption and high yield, and do not produce toxic products or require complex instruments; however, eco-friendly approaches are preferable.[24] Chemical degradation is one of the most extensively utilized strategies for removing pollution from the environment, including ozone/UV, irradiation/H_2O_2 oxidation, photocatalytic degradation, supercritical water oxidation, and electrochemical methods.[25]

Recently, there have been many attempts to build efficient and novel catalytic systems for environmental applications.[26] Also, the use of homogeneous catalysts in industry is a challenge, and thus heterogeneous catalysts are more suitable because of their high stability, recyclability, and simple separation from the reaction media.[27] Metal complexes are widely employed as catalysts for eco-friendly applications.[28–30] Furthermore, the catalytic yield of metal complexes can be improved by increasing their active surface area by decreasing their size to the nanoscale (1–100 nm), causing fascinating properties and differences from bulk materials to emerge.[31,32] Metal nanoparticles (MNPs) such as gold, palladium, silver, platinum, and copper have recently been explored as catalysts for removing organic dyes and nitro chemicals.[33–37]

[a]*Catalysts and Organic Synthesis Research Laboratory, Department of Chemistry, Iran University of Science and Technology, Tehran, Iran*

[b]*Department of Chemistry, Qom Branch, Islamic Azad University, Qom, Iran. E-mail: ma.ghasemzadeh@iau.ac.ir; qasemzade.a@gmail.com*

[c]*Institute of Nano Science and Nano Technology, University of Kashan, Kashan, Iran*

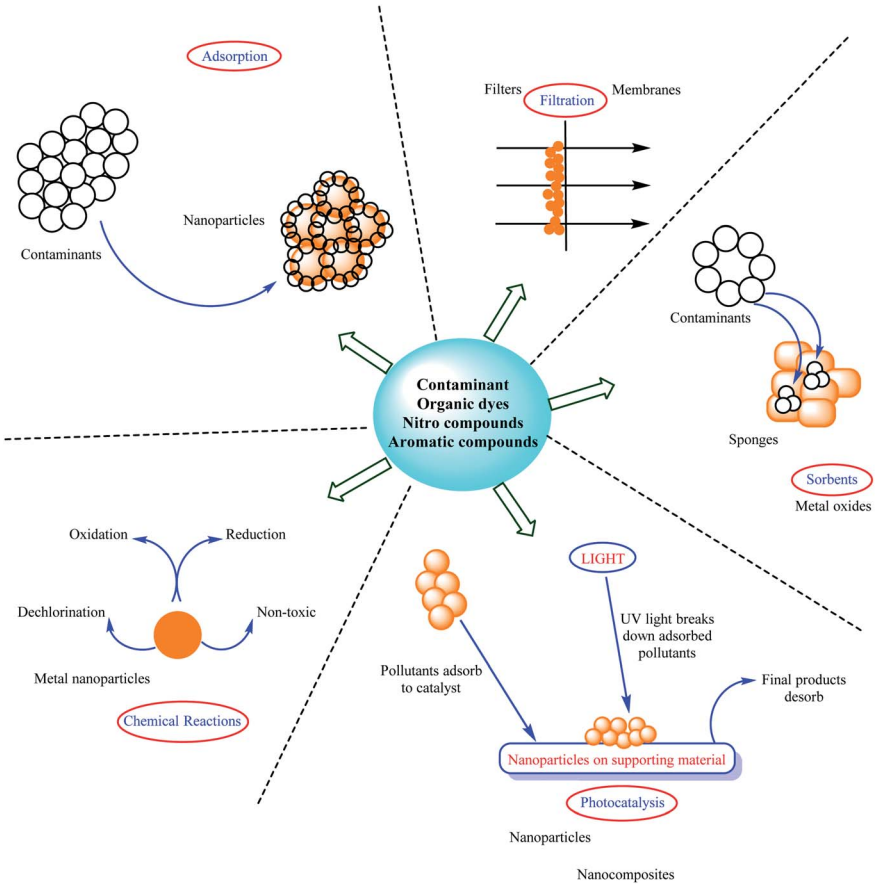

Scheme 1 Different methods employed for environmental remediation.

2. Hydrogel

Hydrogels with three-dimensional networks are insoluble polymeric materials comprised of numerous hydrophilic groups, which can load a vast amount of water. It has been reported that hydrogels are versatile carriers of active compounds including enzymes, drugs, and nanoparticles. Recently, smart hydrogels with the ability to respond to stimulation from the external environment, such as additional chemicals, pH, temperature, and light, have received increasing attention.[38–43] Thus, due to these attractive properties, these smart hydrogels can be potential materials with promising applications in drug delivery, chemical sensors, catalysts, and optics.[44–50]

2.1. Classification of hydrogels

Hydrogels can be divided into numerous types based on their preparation procedure, ionic charge, and physical structures, including homopolymer hydrogels, co-polymer hydrogels, multi-polymer hydrogels, and interpenetrating network hydrogels. Homo-polymer hydrogels are cross-linked networks of hydrophilic monomer units of one type, whereas co-polymer hydrogels, are made by cross linking chains made up of two co-monomer units, one of which must be hydrophilic for them to swell in water. Three or more comonomers are reacted together to form multi-polymer hydrogels. Finally, interpenetrating network hydrogels can be made in two ways, *i.e.*, in a premade network and solution. The typical strategy is the polymerization of one monomer within various cross-linked hydrogel networks. The monomer polymerizes to form a polymer or a second cross-linked network that is intermeshed with the first network.

Hydrogels can also be categorized in a variety of ways. Ionic hydrogels with ionic charges on the backbone polymers are classed as follows: (A) uncharged, (B) anionic hydrogels (containing only negative charges), (C) cationic hydrogels (having only positive charges) and (D) ampholytic hydrogels (having both positive and negative charges). The net charge on these last gels can be harmful, positive, or neutral.

Hydrogels can be characterized as either (A) amorphous hydrogels (with covalent cross-links) or (B) semicrystalline hydrogels, depending on the physicochemical structural properties of their network (may or may not have covalent cross-links). The macromolecular chains in amorphous hydrogels are randomly organized. Alternatively, semicrystalline hydrogels (crystallites) consist of self-assembled regions of organized macromolecular chains.[38–40]

2.2. Preparation of hydrogels

Small multifunctional molecules such as monomers and oligomers are frequently combined, reacting to form a network

structure, for the fabrication of covalently cross-linked hydrogels. Large polymer molecules can sometimes be cross-linked with small multifunctional molecules. The reaction of two chemical groups on two distinct molecules, which can be initiated by catalysts, photopolymerization or radiation cross-linking, can produce this type of cross-linking.

Free radical reactions are used various ways to make cross-linked hydrogels. One approach is a copolymerization-cross-linking reaction involving one or more monomers and one multifunctional monomer in small amounts. Two water-soluble polymers can be cross-linked using a similar mechanism involving the generation of free radicals on both polymer molecules, which combine to create a cross-link. These reactions are known as free radical polymerization or cross-linking reactions. Moreover, they can be triggered by the decomposition of peroxides or azo compounds, or by ionizing radiation or UV light. Ionizing radiation involves the use of gamma rays, X-rays, or electron beams to excite a polymer, causing free radical reactions to generate a cross-linked structure. These free radical reactions, which normally occur in the absence of oxygen or air (note: some polymers are damaged by radiation, especially in air), result in the rapid development of a three-dimensional network.[38]

Chemical cross-linking is another method that involves the reaction of a linear or branched polymer directly with a difunctional or multifunctional low-molecular-weight cross-linking agent. This agent frequently connects two higher-molecular-weight chains through its di- or multifunctional groups. There are several well-known processes for joining hydrophilic polymers together or with cross-linkers to generate hydrogels, including some newer techniques that are gaining traction, such as the Michael addition of dithiol compounds with divinyl compounds. A related method involves the cross-linking of a tiny bifunctional molecule with linear polymeric chains that have pendant or terminal reactive groups such as –OH, –NH_2, NCO, and –COOH. Enzymes can also be used to cross-link natural polymers such as proteins in a similar way.

2.3. Formation mechanism of hydrogels

The different types of gelation mechanisms are summarized in Table 1. Gelation can take place either by physical cross-linking (physical gelation) or by chemical cross-linking (chemical gelation) and radiation cross-linking. Physical gels can be sub-categorized as strong physical gels and weak gels. Strong physical gels have strong physical bonds between their polymer chains and effectively permanent under a given set of experimental conditions. Weak physical gels have reversible links formed from temporary associations between their chains. Alternatively, chemical gelation involves the formation of covalent bonds and always results in a strong gel.[51]

2.4. The techniques for the characterization of hydrogels

To design hydrogels with the desired performance and structure, the determination and characterization of their network parameters are significant. Table 2 presents the techniques for the characterization of hydrogels including physico-chemical, structural and thermal characterization, and the tools for

Table 1 The general methods to produce physical and chemical gels

Physical cross-linking	Chemical cross-linking	Radiation cross-linking
Heating/cooling a polymer	Chemical cross-linkers	Aqueous-state radiation
Ionic interaction	Grafting (chemical grafting and radiation grafting)	Radiation in paste
Complex coacervation		Solid-state radiation (cross-linking in the solid state, natural polymers and synthetic/natural polymer blends)
H-bonding		
Maturation (heat-induced aggregation)		
Freeze-thawing		

Table 2 Techniques for the characterization of hydrogels

Physico-chemical characterization	Structural characterization	Thermal characterization
Solubility	Transmission electron microscopy	Differential scanning calorimetry
Swelling measurement	Scanning electron microscopy	Thermogravimetric analysis
Sol gel analysis	Atomic force microscopy	Dynamic mechanical thermal analysis
Rheology	Dynamic force microscopy	
UV-Vis absorption spectroscopy	Confocal microscopy	
Infrared spectroscopy		
Mass spectroscopy		
Nuclear magnetic resonance		
Light scattering		
X-ray diffraction analysis		

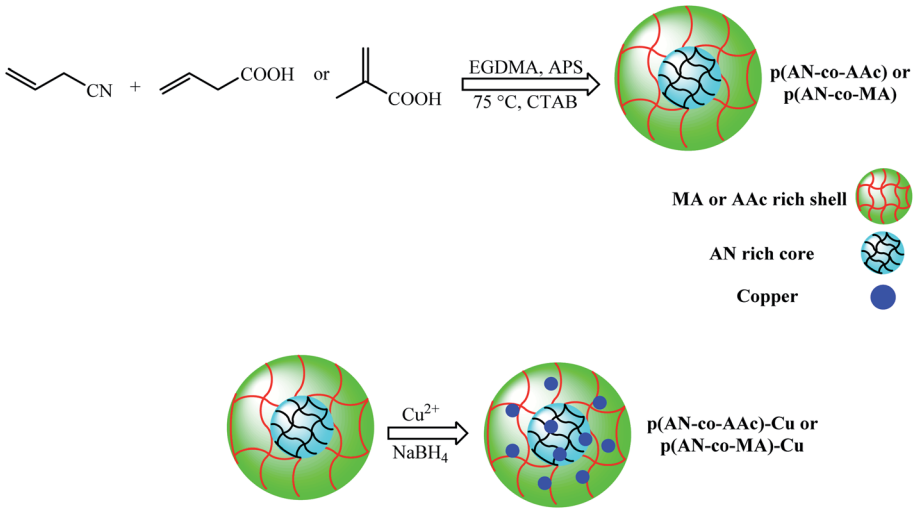

Scheme 2 Preparation of Cu NPs inside p(AN-*co*-MA) and p(AN-*co*-AAc) particles.

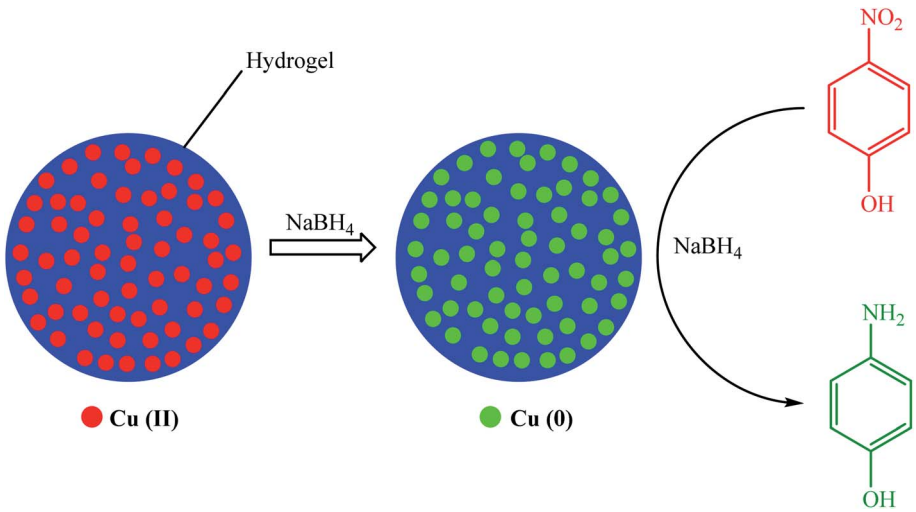

Scheme 3 Schematic of the creation of Cu NPs inside p(AMPS) hydrogel network and their use for the reduction of 4-NP to 4-AP.

their physicochemical characterization such as infrared spectroscopy, atomic force microscopy, X-ray diffraction analysis, electron microscopy, and many other techniques are described to characterize their structure.[52]

2.5. The reaction mechanism for the catalytic reduction/degradation of organic pollutants by hydrogels

Contaminants may be adsorbed on hydrogels through various methods including complexation, coordination, chelation, ion

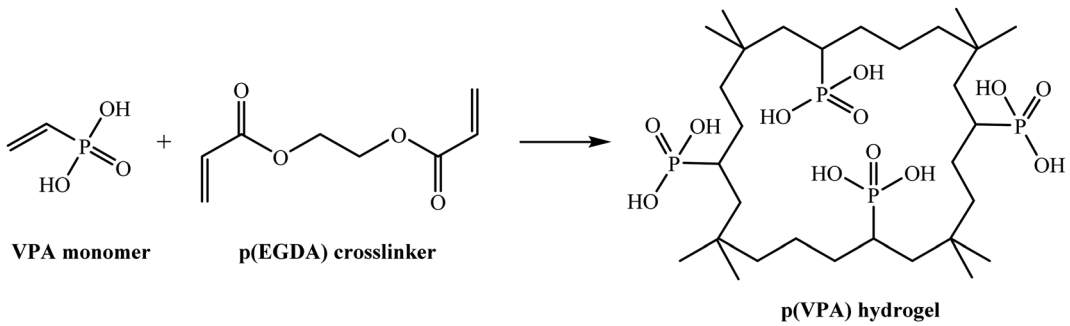

Scheme 4 Bulk p(VPA) hydrogel crosslinking by p(EGDA).

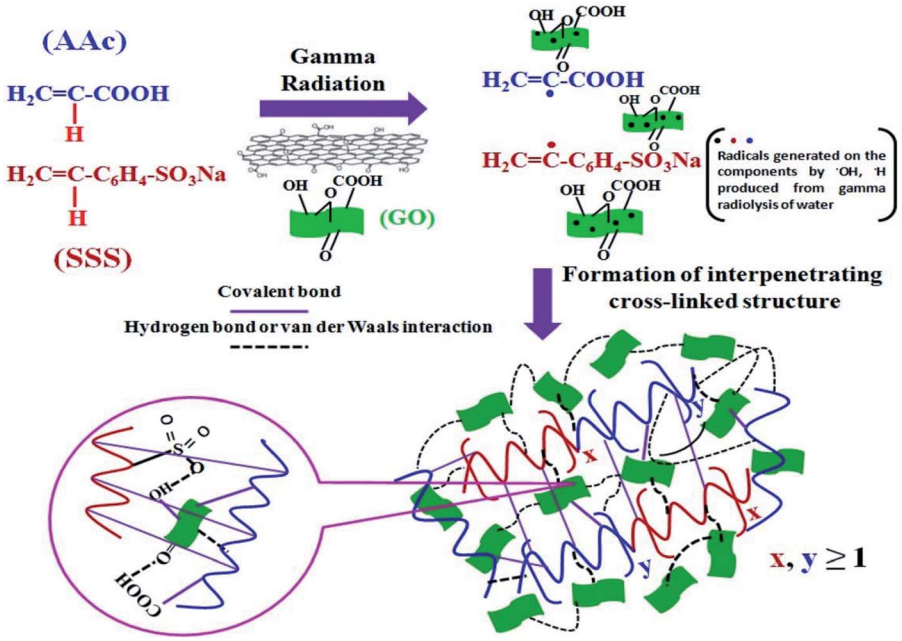

Fig. 1 Preparation of the blended poly(AAc10–SSS15–GO0.01) composite hydrogel *via* a crosslinking process based on gamma radiation. This figure has been reproduced from ref. 83 with permission from John Wiley & Sons Inc. Copyright 5316550528241.

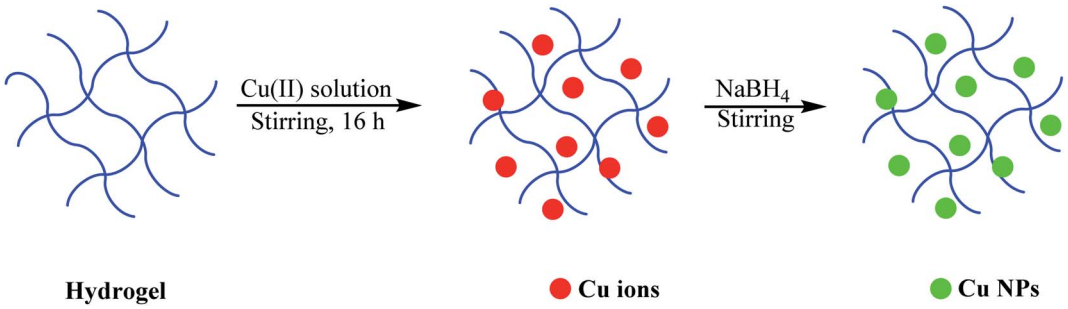

Scheme 5 Synthesis of p(AAc-*co*-AAm)–Cu.

exchange, adsorption by physical forces, and ion trapping in their inter- and intra-fibrillar capillaries.[53] These methods are always influenced by the properties of the hydrogels, the physical and chemical features of the specific type of pollutant being targeted, and the micro-environmental conditions (such as the contact solution pH and ionic strength).[54] Hydrogels have the ability to remove pollutants through a variety of mechanisms or by combining the impacts of several different mechanisms, for example, the reduction of nitrophenols to aminophenols.

The analysis of the reaction mechanism is beneficial for the development of more effective catalysts. An example of a heterogeneous catalytic reaction is the catalytic reduction of nitrophenols using hydrogel-supported metal nanoparticles. The Eley–Rideal and Langmuir–Hinshelwood models can both be used to predict the course of a heterogeneous catalytic reaction. In the case of the Eley–Rideal model, only one of the educts will adhere to the surface of the catalyst and interact with the other educt in the solution. According to the Langmuir–Hinshelwood model, both educts adsorb on the surface of the catalyst and undergo reactions there. Accordingly, by conducting two sets of tests, namely, examining the dependence of the rate constant on the concentration of PNP and sodium borohydride, the appropriate reaction mechanism for the reduction of nitrophenols can be proposed.

In the Eley–Rideal model, the rate increases with an increase in the concentration of PNP, which is not adsorbed on the surface. Alternatively, the rate constant decreases with an increase in the concentration of PNP according to the Langmuir–Hinshelwood model.[55,56]

In the present review, we describe the advantages and properties of copper and palladium-based hydrogels. In addition, the role of copper- and palladium-based hydrogels in the development of novel, safe, and efficient catalysts is explained.

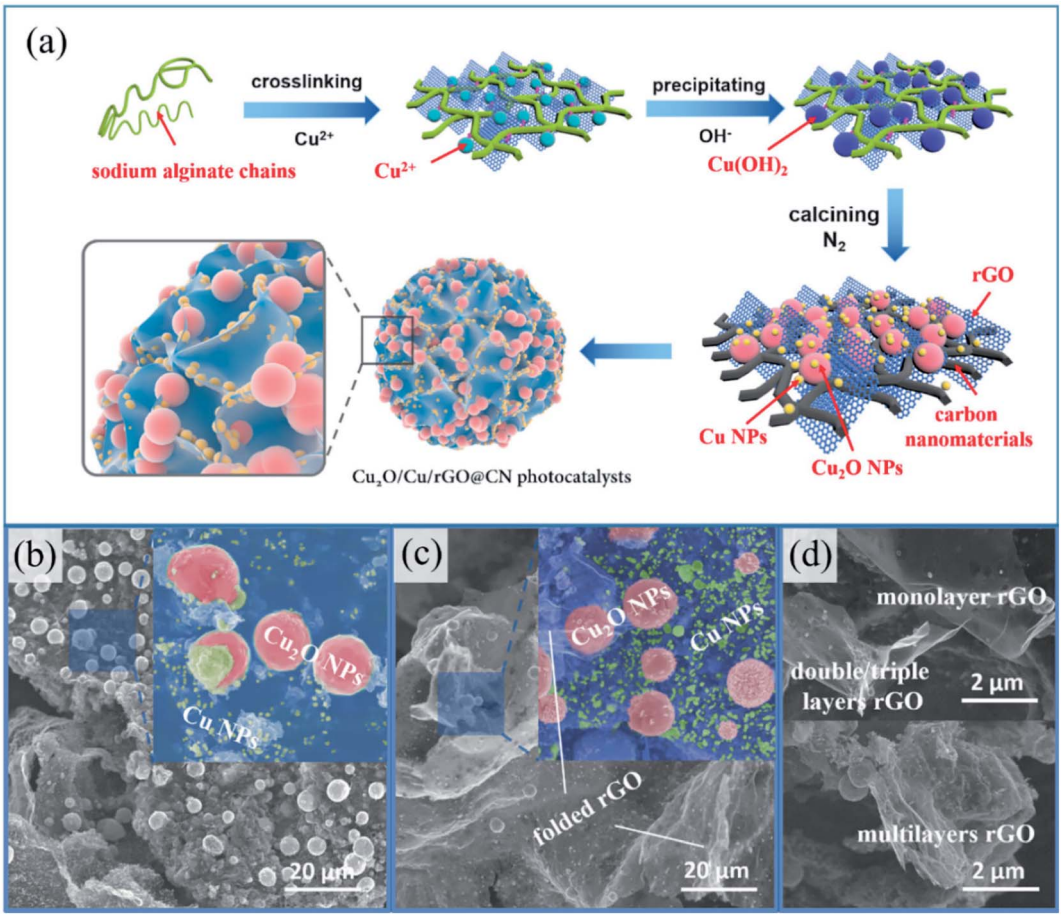

Fig. 2 (a) Formation of Cu_2O/Cu/rGO@CN photocatalysts using sodium alginate hydrogel as a template. SEM images of (b) Cu_2O/Cu@CN, (c) Cu_2O/Cu/rGO@CN-4 and (d) rGO. This figure has been reproduced from ref. 85 with permission from Elsevier. Copyright 5316550031989.

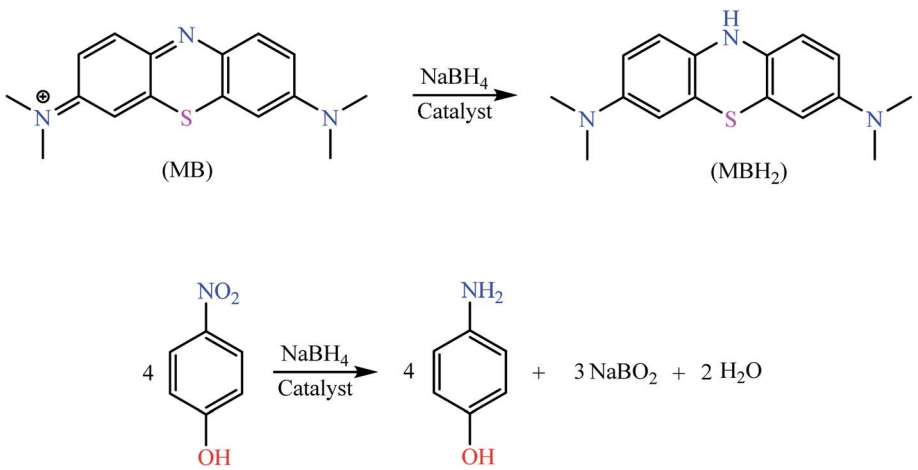

Scheme 6 Chemical reduction of 4-NP and MB.

3. Catalytic applications of synthesized palladium- and copper-based hydrogels

Some hydrogels have a large number of polar functional groups such as hydroxyl and carboxyl groups, which can strongly chelate with transition metals (Au,[57] Ag,[58] Cu,[59] Pd,[60] Ni,[61] Co,[62] *etc.*), leading to the effective loading of metal ions/nanoparticles and preventing their aggregation. Furthermore, they can increase the ion/nanoparticle loading and number of catalytic sites for catalytic reactions. Also, some hydrogels are

biocompatible and biodegradable, and thus can be applied as green, low-cost, and suitable candidates for the removal of pollutants from the environment.[63,64] Generally, nanocomposite hydrogels can be prepared by immersing a hydrogel in aqueous solutions of the respective metal salts. Subsequently, the metal ions are converted to metal nanoparticles *via* reduction by a typical reducing agent, such as $NaBH_4$. Nitro compounds, phenols, and heavy metals are the most common pollutants, and thus an overwhelming number of works has been focused on their destruction.[65–67] Au-,[64] Pt-,[68] and Ag-based[69] hydrogels are commonly used for the catalytic reduction of 4-nitrophenol (4-NP) despite their high cost. Alternatively, copper (Cu) is a good candidate to replace these expensive metals because it is an abundant element in the Earth's crust.[70–75] Also, palladium nanoparticles (Pd NPs) are one of the most promising candidates for pollutant removal due to their outstanding catalytic activity. Thus, among the different transition metals, Pd and Cu nanoparticles or Cu and Pd-based complexes have been significantly used in catalytic applications, especially considering their exclusive features and low cost. Besides, Cu NPs and Pd NPs play critical roles in degrading organic pollutants.[76–79] Recently, Pt- and Cu-based hydrogels have been regarded as active metals with excellent performances for different chemical transformations. Different synthetic (such as polyacrylamide and polyacrylic acid) and natural-based polymers (such as chitosan and cellulose) are used as supports. The purpose of the extensive research in this area is to develop low-cost approaches for the scalable production of biocompatible catalysts. In this section, we present the catalytic uses of these compounds in the degradation of environmental pollutants.

3.1. Reduction and degradation of environmental pollutants using Cu-based hydrogels

3.1.1. Synthetic polymer-based catalysts. In 2011, Sahiner *et al.* reported a facile technique for the synthesis of some polymers with various behaviors, which have a core/shell structure (acrylonitrile (AN) as the core and acrylic acid (AAc) and methacrylic acid (MA) as the shell monomers) through microemulsion polymerization using hexadecyltrimethylammonium bromide (CTAB) as the cationic surfactant (Scheme 2).[80] The prepared nanoparticles exhibited significant potential for use in various fields; firstly, as drug targeting vehicles in the biological field. Secondly, for the removal of organic pollutants such as the toxic organic species 4-nitrophenol (4-NP) and herbicide (Paraquat) in eco-friendly uses, and thirdly as a model for preparing copper catalysts to reduce 4-NP to 4-aminophenol (4-AP). The created p(AN-*co*-AAc) and p(AN-*co*-MA) particles were further chemically modified to make them more hydrophilic by converting their nitrile groups to amidoxime groups. The amidoximated particles presented improved absorption capacity for metal and organic species and enhanced catalytic behaviors.

In 2012, Ozay *et al.* reported a simple route for the preparation of Cu(0) nanoparticles inside p(2-acrylamido-2-methyl-1-propansulfonic acid) (p(AMPS)) hydrogel networks.[81] The p(2-acrylamido-2-methyl-1-propansulfonic acid)–Cu composites were utilized for the reduction of 4-NP as a model reaction in the presence of excess $NaBH_4$, exhibiting superior catalytic activity (Scheme 3). Even in the presence of a significantly lower quantity of catalyst (1.1 mg Cu(0)), the degradation rate of 4-NP by the p(2-acrylamido-2-methyl-1-propansulfonic acid)–Cu composites at a temperature close to room temperature (30 °C) led to a much higher value (0.1032 min^{-1}) compared to Ni(0) and Co(0) catalysts synthesized under very similar conditions. At various activation energies and reaction temperatures, the kinetic parameters defined for 4-NP and 4-AP were 39.2 and 28.2 $kJmol^{-1}$, respectively.

In 2013, Sahiner and Sagbas synthesized bulk poly(vinyl phosphonic acid) (p(VPA)) hydrogels through a photopolymerization method utilizing polyethylene glycol diacrylate with various molecular weights as the cross-linker (Scheme 4).[82] The prepared hydrogel was used as a template for the *in situ* synthesis of Ni, Co, and Cu nanoparticles. Initially, the equivalent ions from aqueous media were loaded in the poly(vinyl phosphonic acid) hydrogel complexes. Subsequently, the metal ions were reduced by sodium borohydride to the (p(VPA)) hydrogel matrices. They investigated the catalytic performance of p(VPA)–M (M: Co, Ni, Cu, *etc.*) for the reduction of 4-NP to 4-AP.

In 2017, Guin and co-workers synthesized a thermally stable mixed elastic poly(acrylic acid–sodium-sulfonate-styrene graphene oxide) (poly(AAc–SSS–GO)) superabsorbent hydrogel *via* addition polymerization induced by free gamma radiation after crosslinking (Fig. 1).[83] The composite material adsorbed 98 mg g^{-1} copper(II) from an aqueous solution of copper(II) at room temperature at pH 5 with the chemi-adsorption of copper(II) ions by its various functional groups with high energy. Through

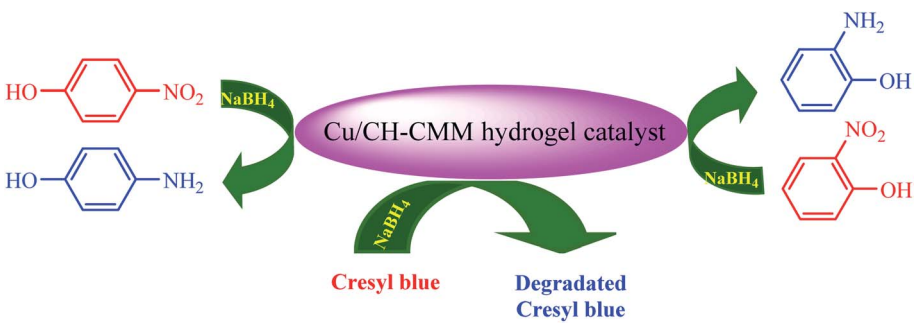

Scheme 7 Degradation of 2-NP, 4-NP and CB by Cu/CS–CMM catalyst.

the chemical reduction of the pre-adsorbed copper(II) ions, Cu NPs with a size of 12 ± 8 nm were prepared *in situ*. They confirmed the excellent catalytic activity of Cu NP–poly(AAc–SSS–GO) for the reduction of 4-NP to 4-AP.

In 2017, Naseer and co-workers synthesized poly(acrylic acid-*co*-acrylamide) (p(AAc-*co*-AAm)) hydrogels, which were subsequently used as templates for the synthesis of Cu nanoparticles (Scheme 5).[84] The Cu NPs were prepared *via* the *in situ* reduction of Cu(II) ions. The synthesized p(AAc-*co*-AAm)–Cu composites were utilized as catalysts for the reduction of 4-NP and as an adsorbent in aqueous media to remove malachite.

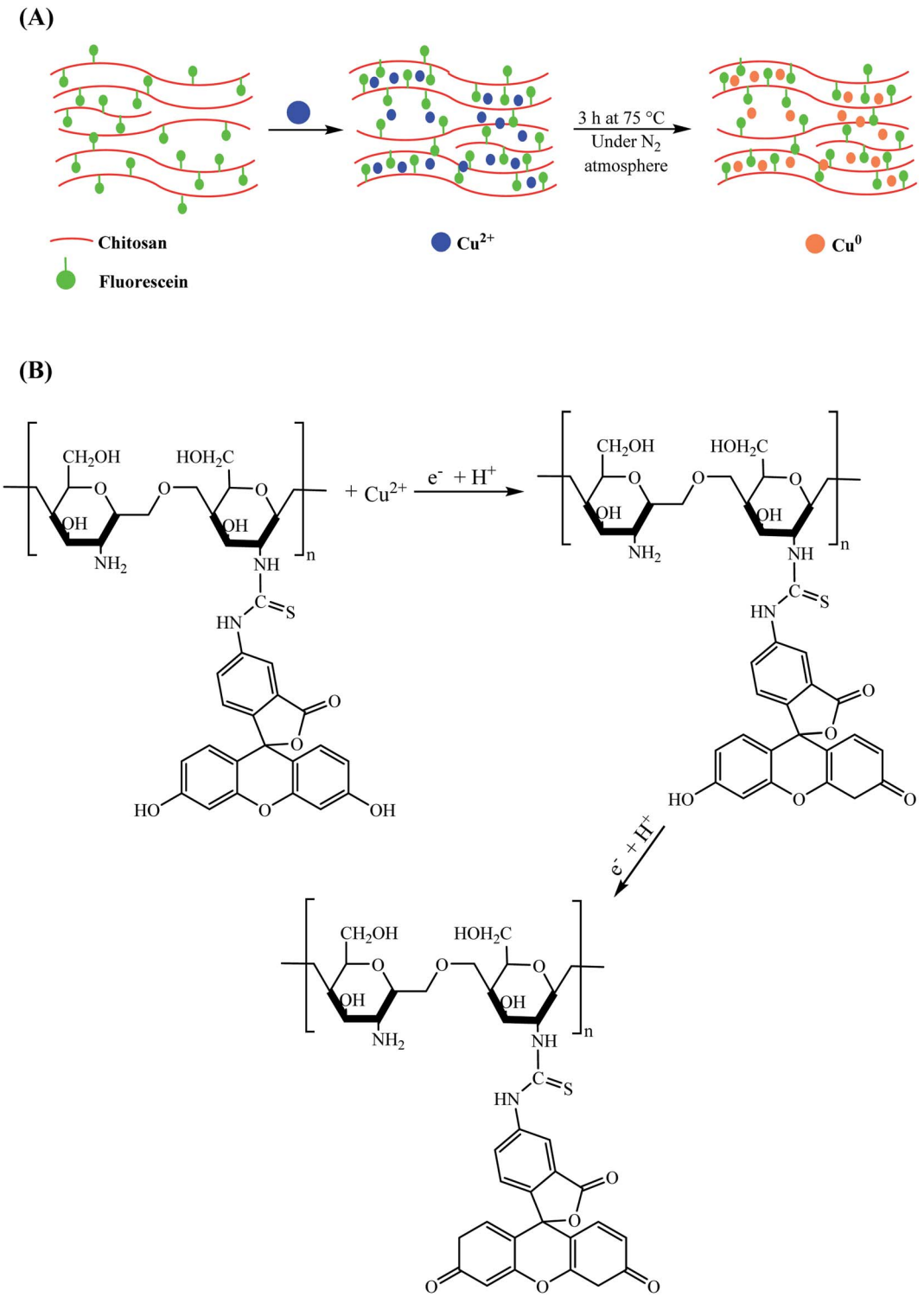

Scheme 8 (A) Preparation of CS/F–Cu film and hydrogel nanocomposites and (B) proposed mechanism for the reduction of Cu^{2+} to Cu^{0}.

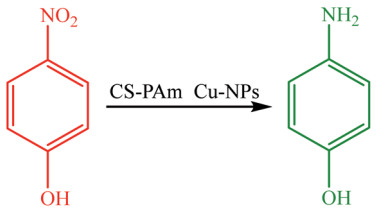

Scheme 9 Reduction of 4-nitrophenol by CS-PAmCu-NP catalyst.

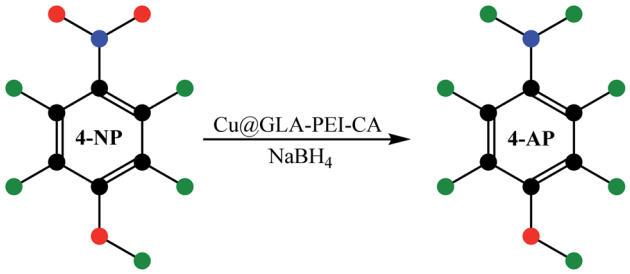

Scheme 10 Reduction of 4-nitrophenol by Cu@GLA–PEI–CA.

Moreover, the p(AAc-*co*-AAm)–Cu catalyst could be reutilized 4 times with no decline in its catalytic activity.

In 2019, Li and colleagues synthesized some Cu_2O/Cu/reduced graphene oxide @carbon nanomaterial (Cu_2O/Cu/rGO@CN) photocatalysts *via* a new sodium alginate hydrogel technique (Fig. 2).[85] Cu_2O NPs (~50 nm) were synthesized *via* a calcination method under the protection of a nitrogen atmosphere. Inevitably, Cu nanoparticles (~6 nm) were found over the surface of Cu_2O. Thus, a Cu_2O/Cu heterostructure was formed, which was identified as a Schottky junction. Synchronously, graphene oxide was reduced *in situ* by sodium alginate during the synthetic procedure, and eventually its 3-D structure contributed to the formation of the hydrogel skeleton. The photocatalytic activity and adsorption capacity of Cu_2O/Cu/rGO@CN improved considerably when it was modified by 3-D rGO. Subsequently, the synthesized Cu_2O/Cu/rGO@CN was employed as an effective catalyst for the degradation of *p*-nitrochlorobenzene. The advantages of this method included facile synthesis, no need for complex instruments, and use of nontoxic raw materials.

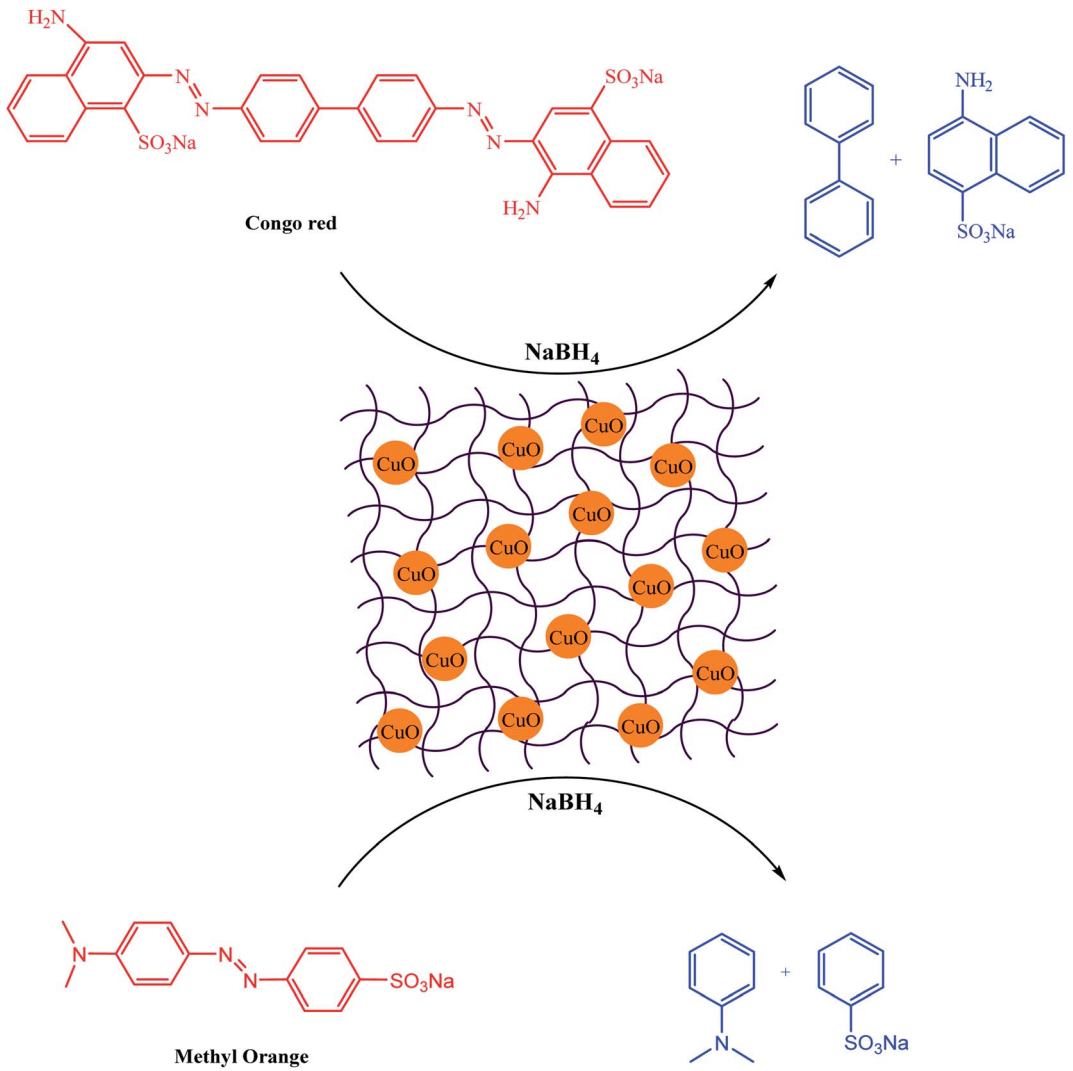

Scheme 11 Reducing methyl orange and Congo red by GL–CuO hydrogel nanocomposite catalyst.

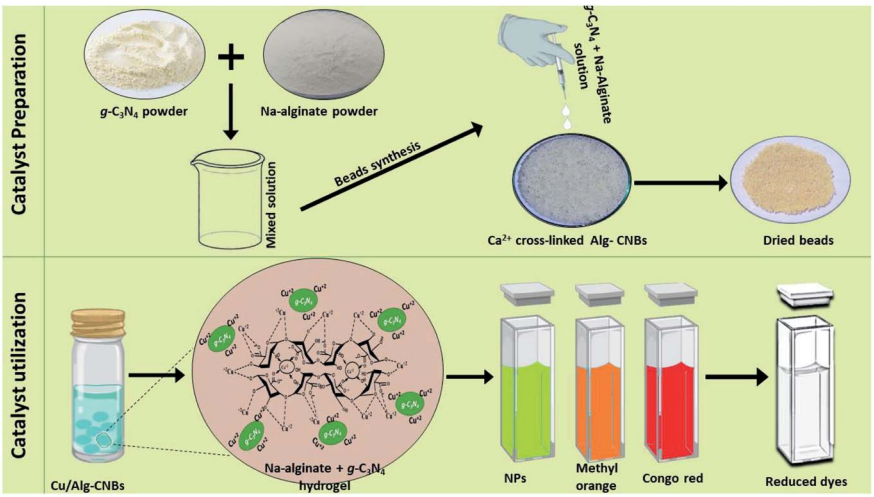

Fig. 3 Preparation of Cu^0/Alg–CNB catalytic beads and their catalytic utilization. This figure has been reproduced from ref. 92 with permission from Elsevier. Copyright 5316550823396.

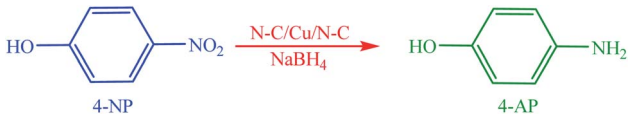

Scheme 12 Reduction of 4-NP in the presence of N–C/Cu/N–C.

Li *et al.* synthesized nanostructures of steady flexible electrospun hydrogel nanofibers comprised of poly(allylamine hydrochloride) and poly(acrylic acid).[86] The metal NPs were formed by loading the hydrogel fibers with metal ions such as Ag and Cu and immersing them in solutions with metal ions after chemical reduction. Finally, the metal ions were absorbed from the medium by the hydrogel fibers. They presented a viscous environment for promoting the creation of alloy particles with a size of less than 25 nm. The reduction of methylene blue (MB) and 4-NP was carried out to examine and compare the catalytic activity of Ag–Cu bimetallic NPs and monometallic NPs (Scheme 6). It was found that the Ag–Cu bimetallic NPs presented desirable selectivity to reduce 4-NP and better catalytic activity for the degradation of MB.

3.1.2. Natural polymer-based catalysts. In 2016, Kamal and colleagues reported a simple method for the preparation of CS–CMM by adhering chitosan (CS) on a cellulose microfiber mat (CMM).[87] The synthesized CS–CMM was utilized as a host for the preparation of Cu NPs. The metal ions encapsulated in the chitosan layer were reacted with $NaBH_4$ for the synthesis of copper NPs loaded on CS–CMM (Cu/CS–CMM), followed by adsorbing copper(II) ions from an aqueous solution of $CuSO_4$. The created Cu/CS–CMM was used as a catalyst for the reduction of the aromatic rings in 2-NP, 4-NP, and the organic cresyl blue dye (CB) (Scheme 7). The rate constants for the reduction of cresyl blue, 2-NP and 4-NP were 1.3×10^{-3} s^{-1}, 1.2×10^{-3} s^{-1}, and 2.1×10^{-3} s^{-1}, respectively.

In the same year, a simple procedure was reported for the synthesis of Cu NPs in a chitosan/fluorescein (CS/F) hydrogel and film matrix by immersing the particular matrix in an aqueous medium comprised of a metallic salt precursor and reducing agent under an N_2 atmosphere at 75 °C for 3 h (Scheme 8).[88] The high catalytic yield of the prepared nanocomposites was demonstrated by reducing methylene blue using N_2H_4 as a reducing agent. According to the experimental results, the order of the degradation reaction of the MB–N_2H_4 system and catalytic activity were strongly dependent on the type of nanocomposite used.

Sharma and colleagues synthesized a non-toxic biocompatible chitosan-based hydrogel nanocomposite with Cu NPs through *in situ* free radical polymerization utilizing acrylamide as the monomer. Chitosan was employed as the substrate, glutaraldehyde as the cross-linking agent, and Cu NPs and ammonium persulphate as the initiator (CH–PAmCu–NP catalyst).[89] They employed the prepared hydrogel nanocomposite as a recyclable catalyst with high efficiency for the reduction of 4-NP to 4-AP (Scheme 9).

In 2018, Xiao and co-workers established an internal solidification procedure induced by a rigid template for the preparation of ultrafine MNPs immobilized on calcium alginate, polyethylene imine, and glutaraldehyde beads (Cu@GLA–PEI–CA). During the synthetic procedure, $CaCO_3$ nanoparticles with bi-functional properties were applied as a hard skeleton for adjusting the structure of the catalyst and also as a subsidiary cross-linking agent to obtain hydrogel beads.[90] Copper nanoparticles with a narrow size distribution of 2–3 nm were homogeneously supported on the surface of the GLA–PEI–CA beads with a well-developed hierarchical pore structure and high specific surface area. They observed that the Cu@GLA–PEI–CA beads demonstrated good catalytic activity for the reduction of 4-NP to 4-AP with sodium borohydride in aqueous solution (Scheme 10). Furthermore, this catalytic system could be simply separated and reused.

In 2020, a new bionanocomposite of gelatin as a polypeptide hydrogel comprised of CuO nanomaterial (GL–CuO) was

synthesized by Ahmad and co-workers.[91] After their dispersal, the synthesized CuO NPs were cross-linked with the addition of a CH_2O solution in the GL aqueous solution. The synthesized GL–CuO with an average size of about 60–80 nm showed durable and extraordinary activity for the reduction of Congo red (CR) and methyl orange (MO) in an eco-friendly medium (Scheme 11). This method had the advantages of simple catalyst synthesis, high efficiency, and easy work up.

In 2020, a simple route was reported by Kamal *et al.* for the preparation of carbon nitride (g-C_3N_4)-incorporated sodium alginate (Alg) beads. The Alg–CNBs (alginate carbon nitride beads) were synthesized by adding an Alg aqueous solution containing dispersed g-C_3N_4 to an aqueous solution containing calcium(II) ions (Fig. 3).[92] Then, Alg–CNBs were further treated with various transition metal salt solutions. Subsequently, employing sodium borohydride as a potent reducing agent, the transition metal ions covering the surface of Alg–CNBs were reduced to the zero-valent state (M^0) and utilized for the catalytic degradation of various organic dyes. Finally, the synthesized M^0/Alg–CNBs (where M^0 = Ag^0, Fe^0, Cu^0, and Ni^0) catalysts were examined for the reduction of 4-NP to determine the best one. Among them, it was found that Cu^0/Alg–CNBs reduced 4-nitrophenol to 4-aminophenol efficiently. Also, Cu^0/Alg–CNBs was further employed for the reduction of CR, MO, 2-NP and 2,6-DNP.

In 2021, Xiao *et al.* successfully prepared an N-doped sandwich-like carbon layer coating on copper NPs supported on N-doped porous carbon (N–C/Cu/N–C) by the deposition of a polydopamine (PDA) layer over alginate-based hydrogel beads after high-temperature pyrolysis in N_2.[93] The results demonstrated that copper nanoparticles with a narrow size distribution in the range of 10–30 nm were immobilized uniformly over the porous carbon bead framework by protecting the outer N–C layer. Moreover, the mechanical strength was enhanced effectively by the layer extracted from PDA on the porous beads, therefore preventing the loss of copper NPs during the catalytic reaction. Subsequently, the performance of the prepared catalyst (N–C/Cu/N–C) was assessed for the reduction of 4-NP to 4-AP (Scheme 12).

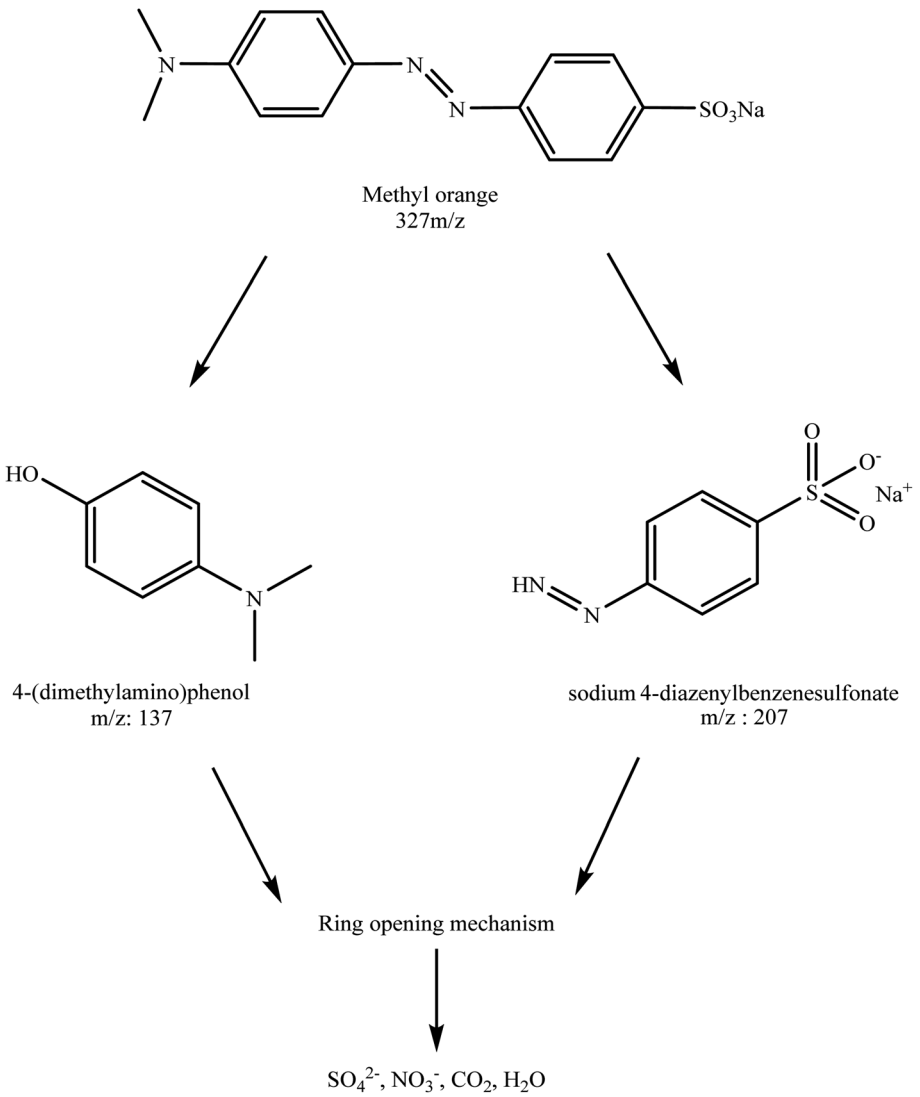

Scheme 13 Proposed degradation path for MO utilizing Cu_2O/TiO_2/CNF/rGH.

In 2022, Andou and co-workers designed a facile method for the *in situ* preparation of a new three-dimensional photocatalyst comprised of Cu_2O/TiO_2 supported on a cellulose nanofiber (CNF)/reduced graphene hydrogel (rGH) through a simple freeze-drying and hydrothermal treatment.[94] The three-dimensional macrostructure acted as an appropriate template for anchoring TiO_2 and Cu_2O, providing an effective electron transport path to improve the photocatalytic activity. According

Table 3 The catalytic elimination of inorganic/organic contaminants utilizing Cu-based hydrogels

Cu-based hydrogels	Size of Cu nanoparticles	Application	Catalytic activity/benefits	Year	Ref.
Cu NPs inside p(AN-*co*-MA) and p(AN-*co*-AAc) particles	—	Reduction of 4-NP to 4-AP	Multipurpose	2011	80[a]
p(AMPS)–Cu	30–35		High conductivity	2012	81[a]
p (VPA)–M	—		Potential applications in bone mineralization	2013	82[a]
Cu NW–Ag (CuAg-3)	100		Superior catalytic activity	2014	96
DNA–Cu-hydrogel	2–3		Potential for green organic synthesis in aqueous media and for biomedical *in vivo* applications Clean synthesis of the catalyst	2016	100
Cu NP–poly(AAc–SSS–GO)	12		Economically viable	2017	83[a]
CH/f-Cu hydrogel	—		Utilized 4 times with no loss in catalytic activity	2017	88[a]
p(AAc-*co*-AAm)–Cu	—		Separable with a magnetic field	2017	84[a]
CH–PAmCu–NPs	—		Good chelation with Cu NPs Multi-functional Selective adsorption and recycling copper element for waste disposal industry	2017	89[a]
Cu NPs-loaded SPI/PEI	10–80		Retained 70% activity after being stored for 30 days	2017	101
WSC-*g*-PAA/PVA–Cu	20–30		Beyond 90% conversion in 10 cycles Tunable structure and properties	2017	102
Cu@GLA–PEI–CA beads	2–3		Cost-effective and biocompatible	2018	90[a]
Cu NP-impregnated cellulose	4–16		Scalable reduction and reusable for 6 times	2019	112
Chitosan–Cu	—		Enhanced mechanical strength and stability	2020	110
Alg–CNB beads	—			2020	92[a]
N–C/Cu/N–C	10–30			2021	93[a]
Cu/CHCMM	48	2-NP, 4-NP and cresyl blue	Economical and environmentally friendly	2016	87[a]
Cu_2O/Cu/rGO@CN photocatalysts	~6	Degradation of *p*-nitrochlorobenzene	Suitable chemical stability during recycling	2019	86[a]
GL–CuO	83	Reduction of Congo red and methyl orange	Good catalytic reduction properties toward different environmental pollutants and easy separation through filtration	2020	91[a]
p(EP-*g*-AA)–Cu	100	Reduction of MB and 4-NP	Maintained 80–90% catalytic activity after 5 times use and 30 days storage	2018	103
poly(allylamine hydrochloride) and poly(acrylic acid) nanofibers	<20		Simplicity, controllability, and versatility	2021	86[a]
Cu(II)–poly(EGDE–DA)	—	Reduction of MO	Oxidation of pharmaceutical product (epinephrine)	2014	97
Cu_2O/TiO_2/CNF/rGH	4.3–6.3		Enhanced photoactivity	2021	94[a]
PEI–Cu	—	Reduction of 4-NP and 2-NP	Very fast reduction times of 1.2 and 0.67 min to 4-AP and 2-AP, respectively	2015	99
Amid–p(Mac–Cu–AN)–M	10–50	Reduction of 4-NP, 2-NP, MO, MB, eosin Y	Individual and simultaneous degradation of cationic/anionic dyes double triple compounds	2016	95
Amid–p(AAm)–Cu	—	Reduction of 4-NP, 2-NP, MB, eosin Y	Fast response to external stimuli, good mechanical strength, and durability	2015	98
WSC-*g*-PAA/PVA–Cu	20–50	Degradation of chloramphenicol	Great potential for future applications for heavy metal recovery and reuse	2018	104
m-WSC/FP–Cu	2–5	Reduction of 2-aminobenzoic acid	Maintained 99.02% over 5 cycles utilization and 90.60% after 30 days storage	2019	105
AG–CuO	15–92	Reduction of 4-NP, 2-NP, 2,6-DNP	Easy recyclability and high catalytic activity	2019	106
BSA–Cu	—	Reduction of 4-NP, CR, MB	Robust hydrogel incorporating metal ions	2020	107
Fe_3O_4–CuO@C	—	Reduction of MB	Enhanced photocatalytic activity	2020	108
Cu/MC	25	Reduction of 4-NP and rhodamine B	Magnetic responsiveness to an external magnetic field	2020	109
CuS@CNs	5	2,4-Dichlorphenol	Improved the separation of photogenerated charge carriers	2021	111

[a] Discussed in the review.

to their findings, TiO_2 and Cu_2O were homogeneously incorporated in the aerogel template, resulting in structures with a larger surface area in the uncovered active sites. In comparison to the bare rGH, Cu_2O/CNF/rGH, CNF/rGH, and TiO_2/CNF/rGH, Cu_2O/TiO_2/CNF/rGH presented enhanced activity for the removal of methyl orange (Scheme 13).

The reports on the use of Cu-based hydrogels for environmental remediation are presented in Table 3.

3.2. Reduction and degradation of environmental pollutants using Pd-based hydrogels

3.2.1. Synthetic polymer-based catalysts. In 2014, a facile technique was reported by Wang *et al.* for the synthesis of a novel bifunctional nanocatalyst composed of 3D macroscopic carbon nanotube (CNT)–graphene hydrogel (GH) supported palladium NPs (Pd–CNT–GH) and its application for the catalytic reduction of 4-NP to 4-AP (Scheme 14).[113] A facile and one-pot self-assembly method was used to synthesize three-dimensional Pd–CNT–GH *via* the hydrothermal treatment of a precursor mixed aqueous solution containing graphene oxide (GO), $PdCl_4^{2-}$, and CNT. Under suitable conditions, the spontaneous redox reaction between the precursor CNT–GO and

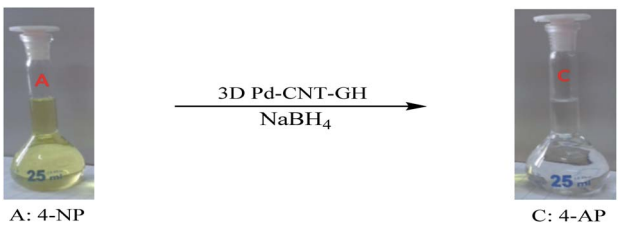

Scheme 14 Reduction of 4-NP in the presence of 3D Pd–CNT–GH.[113]

Scheme 15 Reduction of 4-NP in the presence of rGSs/Fe_3O_4–Pd.

$PdCl_4^{2-}$ occurs simultaneously with the self-assembly of macroscopic CNT–GH, resulting in the formation of three-dimensional Pd–CNT–GH. The catalytic process was accomplished within about 30 s utilizing this catalyst at room temperature. Furthermore, the catalyst could be reused 20 times without considerable loss in its catalytic activity.

In 2017, Shen and colleagues designed and synthesized new three-dimensional graphene oxide nanosheets reduced by molybdenum disulfide and supported by Pd (Pd/MoS_2–rGO) through a convenient one pot self-assembly process (Fig. 4).[114] The restacking of rGO nanosheets was prevented by the presence of MoS_2 and their specific surface area increased. Moreover, a further transport platform was also afforded for palladium NPs to enhance their catalytic features. Excellent catalytic activity for the reduction of 4-NP to 4-AP was demonstrated by the synthesized Pd/MoS_2–rGO NPs in water in the presence of borohydride.

In the same year, Wu and co-workers utilized a two-step technique to synthesize a reduced graphene oxide nanosheet/magnetite–palladium (rGSs/Fe_3O_4–Pd) aerogel with superior recyclability and catalytic performance.[115] In the first step, graphene oxide nanosheet hydrogels were prepared *via* the self-assembly of GSs during the hydrothermal procedure. Meanwhile, the palladium nanoparticles (NPs) and hematite (α-Fe_2O_3) were synthesized and anchored on the hydrogel surface.

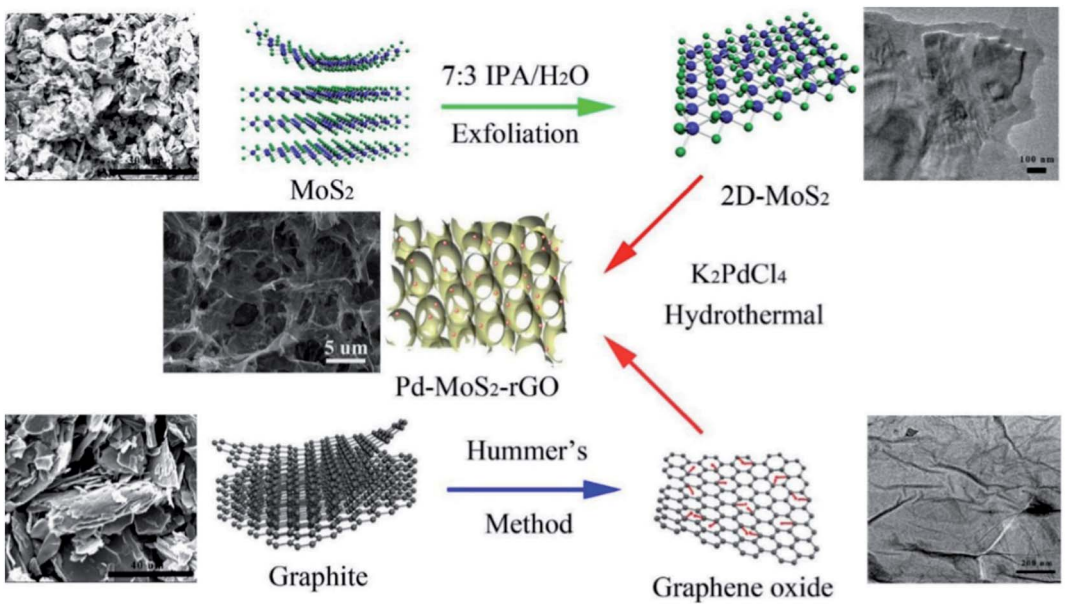

Fig. 4 Procedure for the preparation of the 3D Pd/MoS_2–rGO composite hydrogel. This figure has been reproduced from ref. 114 with permission from Elsevier. Copyright 5316560270510.

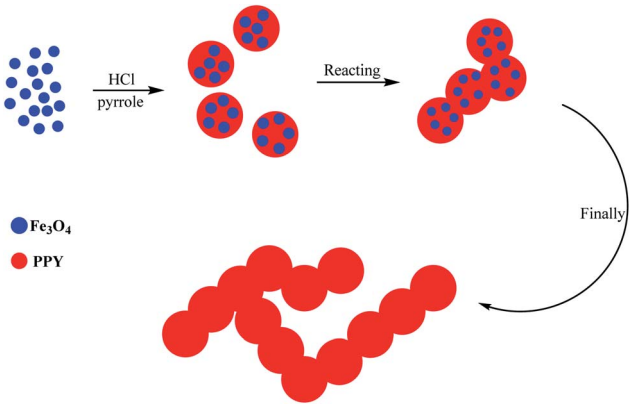

Scheme 16 Possible mechanism for the formation of PPy hydrogel.

Subsequently, upon heat-treatment, the graphene oxide nanosheets were reduced to rGSs, whereas the nonmagnetic α-Fe_2O_3 NPs changed to magnetite Fe_3O_4 nanoparticles. The as-achieved rGSs/Fe_3O_4–Pd aerogel possessed a 3D interconnected porous hierarchical architecture rich in macro-pores and mesopores. This structure was appropriate for catalysis because it not only enhanced the transport and mass diffusion but also simply exposed the catalytic palladium nanoparticles to the substrates. The potential catalytic performance of the synthesized Pd NPs was demonstrated for the reduction of 4-nitrophenol (Scheme 15).

In 2018, Yao and co-workers synthesized a nanobead-based polypyrrole (PPy) hydrogel *via* a reactive-template technique in one step (Scheme 16).[116] Fe_3O_4 NPs were chosen as the reactive template and used as the oxidant for initiating the polymerization of the pyrrole monomer and also guiding the growth of

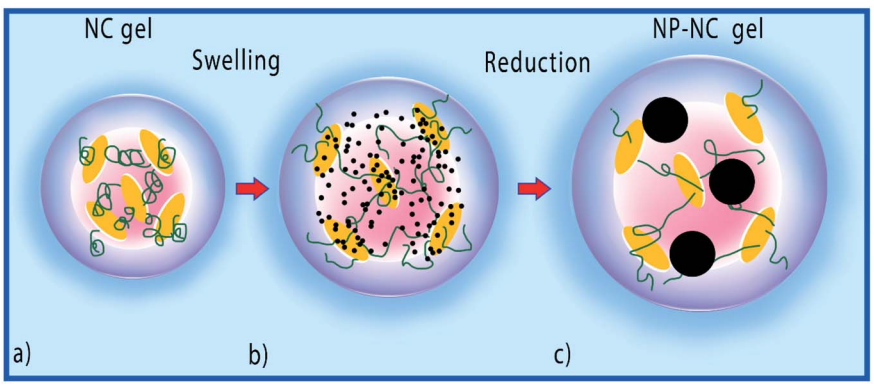

Fig. 5 Schematic showing the formation of the hybrid NP–NC gel: (a) metal ions penetrate the NC gel, (b) metal ions interact with the silanol groups on the clay surface, and (c) metal NPs are formed by the ascorbic-acid reduction of ions, which are subsequently trapped near the clay surface.

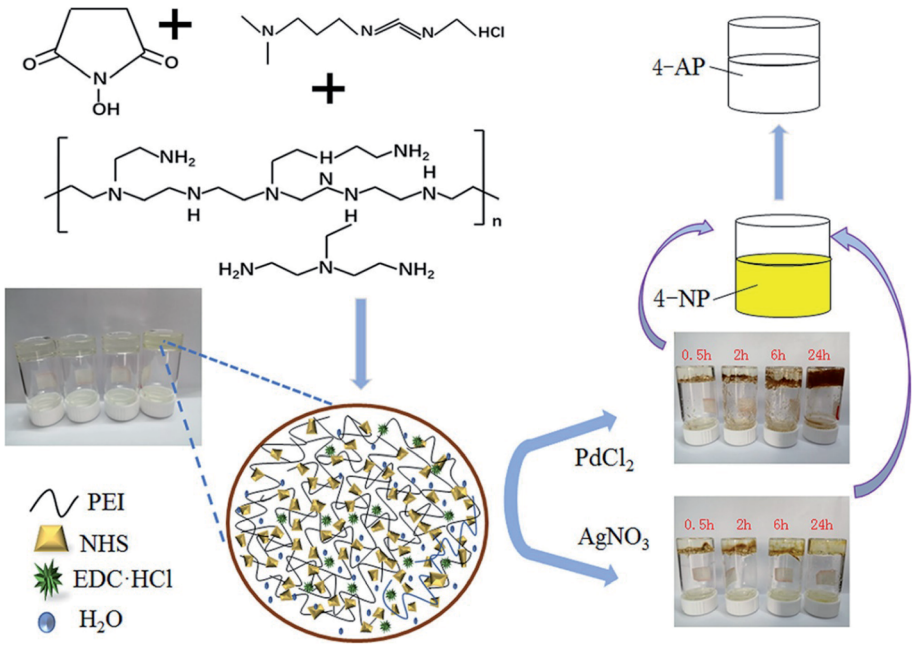

Fig. 6 Preparation and catalytic application of PEI–Ag/PEI–Pd composites and PEI hydrogel.

the polymer chains. Given that the PPy hydrogels were formed by the cross-linking of the individual nanobeads, they bridged the macro-dimension and nano-dimension; thus, a three-dimensional hierarchical porous structure was formed. The PPy hydrogels possessed a large surface area and several interconnected channels, and by taking advantage of their structural merits, they acted as superior candidates for adsorbing rhodamine B. The PPy hydrogels for loading Pd nanoclusters could serve as a support and used as adsorbents.

In the same year, Haraguchi and Varade described a novel approach to prepare discrete monometallic (silver, gold, and palladium) and bimetallic (Au–Pd, Pt–Pd) nanoparticles using a nanocomposite hydrogel comprised of a polymer–clay network (Fig. 5).[117] Thermo-responsive nanocomposite hydrogels (NC gels) were prepared *via* the *in situ* free radical polymerization of *N*-isopropylacrylamide in the presence of clay (synthetic hectorite) nanosheets (CNSs). Given that the CNSs have robust affinities for metal ions, the concentration of the surrounding metal precursors was balanced and non-aggregated and well dispersed. Spherical bimetallic and monometallic NPs were obtained by reducing metal ions using ascorbic acid in NC gels, which were strongly immobilized in the polymer–clay network. The resultant hybrid NP–NC gels, which contained monometallic or bimetallic nanoparticles, exhibited high catalytic activities for the reduction of NP to AP.

In 2020, PEI–Pd and PEI–Ag composite hydrogels were successfully synthesized by Jiao *et al.*[118] Furthermore, the prepared PEI–Pd and PEI–Ag showed extraordinary and durable

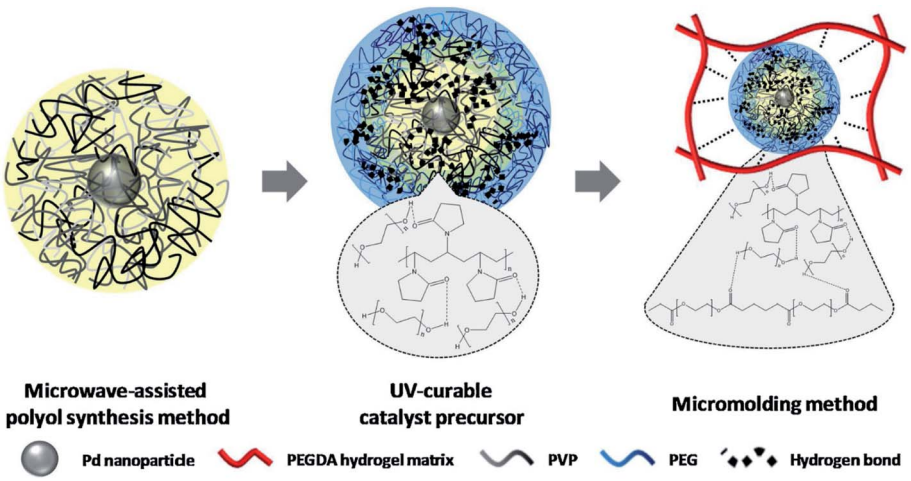

Fig. 7 Postulated stabilization mechanism for Pd NPs immobilized on hydrogels. This figure has been reproduced from ref. 119 with permission from Elsevier. Copyright 5318331364158.

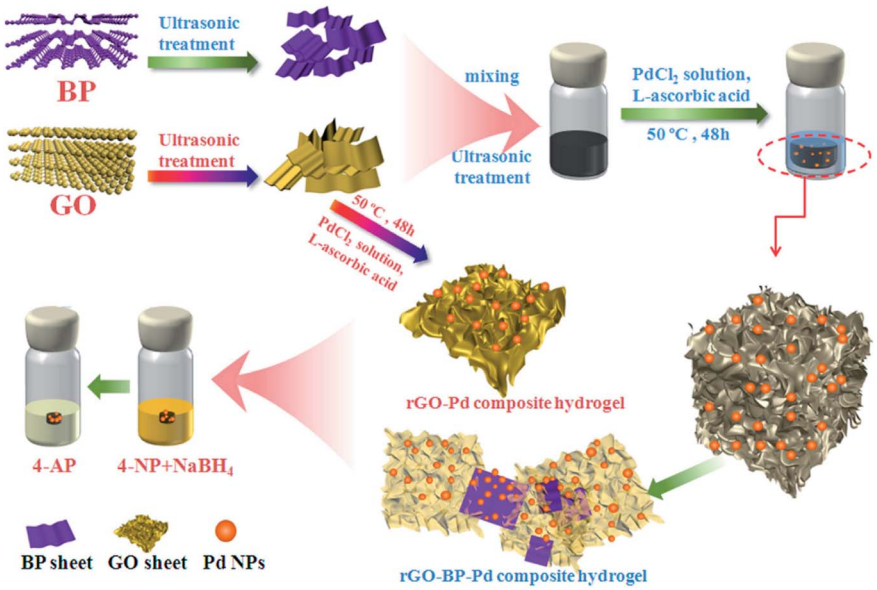

Fig. 8 Catalytic performances and process for the synthesis of rGO-based composite hydrogels. This figure has been reproduced from ref. 120 with permission from Elsevier. Copyright 5318330689362.

activity for the reduction of 4-nitrophenol to 4-aminophenol in an environmentally friendly medium (Fig. 6). This process has many advantages such as the high effectiveness of the composite hydrogels, simple process, and easy workup.

Lee and co-workers described a simple technique for immobilizing palladium NPs with high physicochemical stability in uniform hydrogel microparticles. Simultaneously, it resulted in the high physicochemical stability and dispersion of the immobilized palladium nanoparticles inside the hydrogel microparticles. The PVP (polyvinylpyrrolidone)-stabilized palladium nanoparticles were synthesized *via* a microwave-assisted method. The palladium nanoparticles were immobilized utilizing a micro-molding approach in the UV enhanced hydrogel precursor.[119] The immobilized palladium nanoparticles were physically stabilized because they were trapped in the porous hydrogel framework. Meanwhile, they were chemically stabilized by the H-bonding induced among the PEGDA (polyethylene glycol diacrylate) hydrogel matrix, PVP, and PEG (Fig. 7). Also, the stability of the immobilized palladium nanoparticles against oxidation was

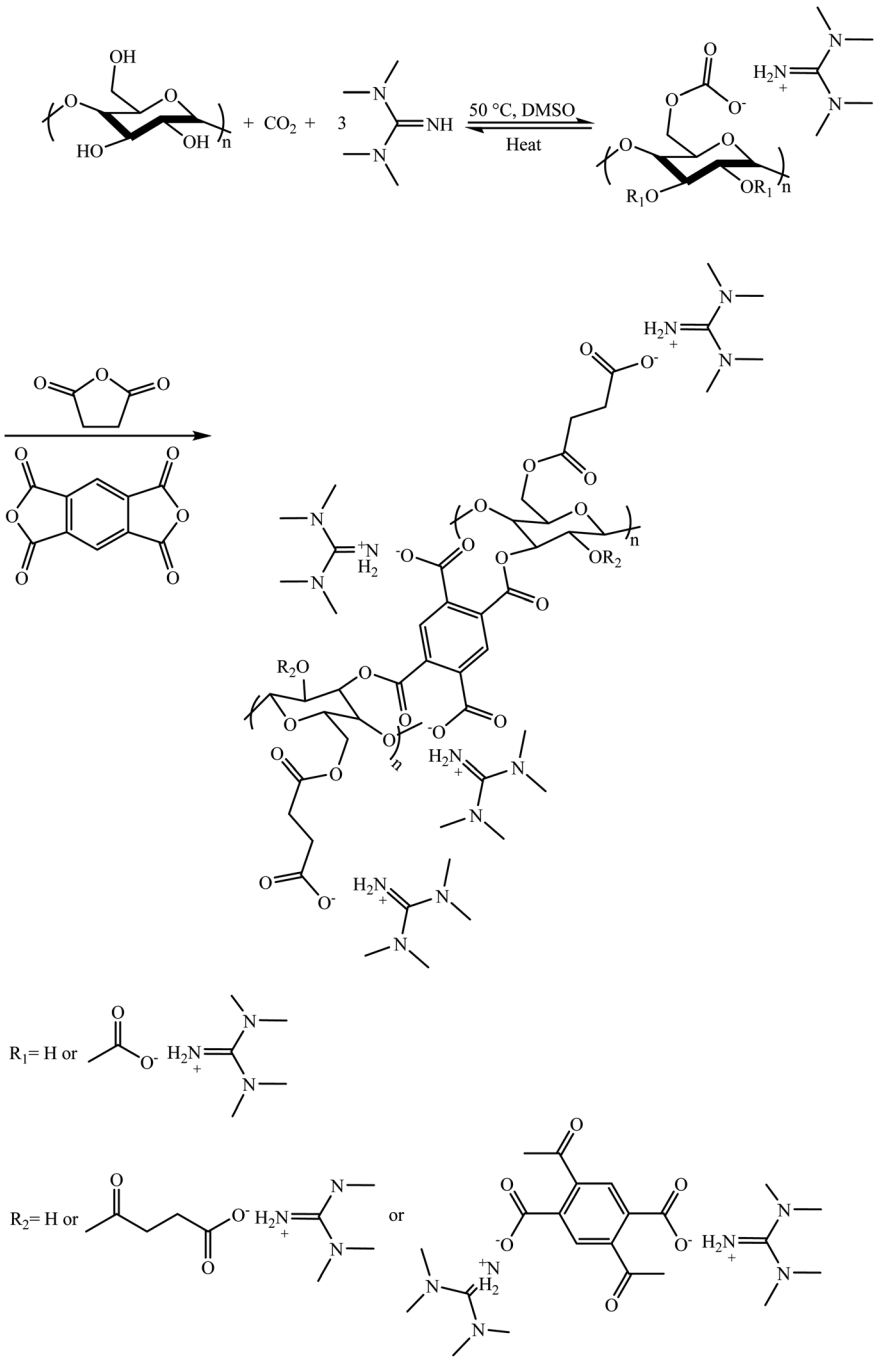

Scheme 17 Synthesis of cellulosic hydrogel anchoring 1,1,3,3-tetramethylguanidine poly-ionic liquid moiety.

confirmed by the formed hydrogen bonding. They investigated the catalytic performance of the synthesized Pd NPs for the reduction of 4-NP to 4-AP.

In the same year, Wang and colleagues synthesized Pd-immobilized rGO and black phosphorus nanosheet-based (rGO–BP–Pd) hydrogels *via* a facile self-assembly method.[120] Precisely, GO was reduced to the rGO hydrogel by addition of L-ascorbic acid. Furthermore, the rGO hydrogel was utilized as a skeleton for loading palladium nanoparticles and the catalytic features of the obtained template hydrogels were investigated (Fig. 8). They also investigated the effects of the hydrogels prepared by adding various quantities of black phosphorus nanosheets (BPNS) on the catalytic reduction of 4-nitrophenol. The outcomes demonstrated that increasing the quantity of BPNS could improve the catalytic activity owing to the interaction between Pd NPs and BPNS.

3.2.2. Natural polymer-based catalysts. In 2019, Xie and colleagues prepared a novel cellulosic hydrogel anchoring a 1,1,3,3-tetramethyl guanidinium–cellulose-based ionic liquid moiety (GC) by simply adding bicyclic anhydrides to the recently established 1,1,3,3-tetramethyl guanidine/DMSO/CO_2 solvent system for cellulose (Scheme 17).[63] The amount and presence of bicyclic anhydrides as a cross-linker were demonstrated to be a key factor for the formation of the hydrogel. Then, the palladium NPs@GC structure was formed by reducing the absorbed palladium(II) ions on GC using sodium borohydride as a reducing agent. The CS provided decent immobilization capacity for palladium nanoparticles, and the obtained Pd NPs@GC presented good reusability and high catalytic performance for the degradation of 4-NP in H_2O.

In the same year, Park and co-workers assessed the catalytic efficiency of alginate hydrogels as a support for catalysts.[121] An alginate solution comprised of magnetite NPs and Pd was continuously dropped *via* a tapered glass capillary utilizing a syringe pump, and the created alginate droplets were gathered in an aqueous solution containing divalent cations. The created Pd NP/MNP-embedded alginate particles were considered as the catalyst support, catalyst, and magnetic stirrer for the reduction of 4-NP (Scheme 18). It was found that the catalytic reactions depended on the magnetic stirring of the alginate hydrogels.

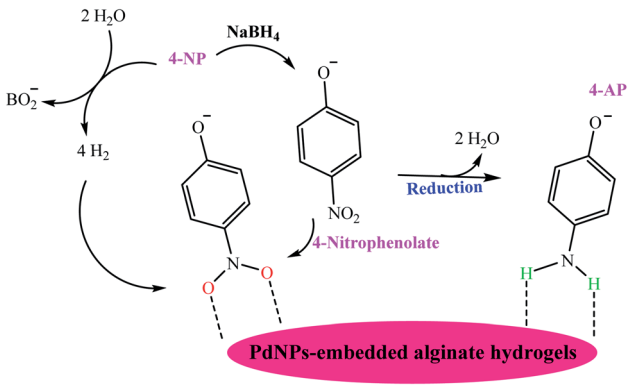

Scheme 18 Reduction of 4-NP to 4-AP applying Pd NP-embedded alginate hydrogel.

In 2020, Jiao and co-workers synthesized a series of palladium NP-incorporated chitosan (CS)-based composite hydrogels by adding carbon nanotubes, graphene oxide, and layered double hydrotalcites (LDHs) to a CS hydrogel with glutaraldehyde as the cross-linking agent and *in situ* growth of palladium nanoparticles.[122] The catalytic reduction of 4-nitrophenol was carried out to evaluate the performance of the chitosan-based composite hydrogel (Scheme 19). The prepared chitosan-based composite hydrogel catalysts presented a higher catalytic performance in comparison with the chitosan hydrogel catalyst-doped palladium nanoparticles (CS-PdNPs) and recoverability for reducing 4-NP in aqueous media. Furthermore, the chitosan-based composite hydrogel catalysts comprised of CNTs possessed the highest catalytic activity among the three types of chitosan-based composite hydrogel catalysts because

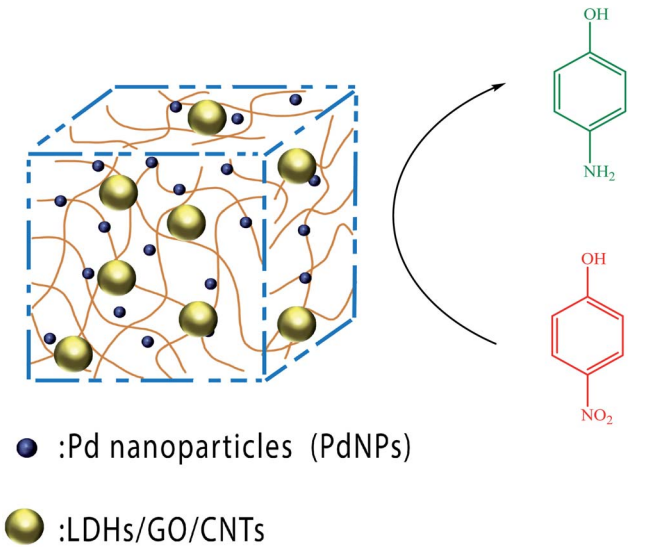

Scheme 19 Reduction of 4-NP to 4-AP applying Pd NPs. This figure has been reproduced from ref. 122 with permission from Elsevier. Copyright 5316560975161.

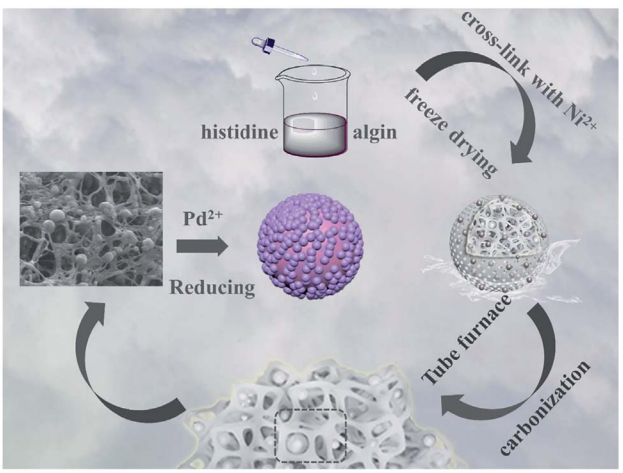

Fig. 9 Synthesis of Pd Ni–N@C. This figure has been reproduced from ref. 123 with permission from Elsevier. Copyright 5357550496279.

Table 4 The catalytic elimination of inorganic/organic contaminants utilizing Pd-based hydrogels

Pd-based hydrogels	Size of Cu nanoparticles	Application	Catalytic activity/benefits	Year	Ref.
Pd–CNT–GH	2–3	Reduction of 4-NP to 4-AP	Catalyzation over about 30 s at room temperature	2014	113[a]
Pd/MoS_2–rGO	5		Catalyzation within 30 s and 20 successive cycles without obvious deactivation	2017	114[a]
rGSs/Fe_3O_4–Pd	—		Magnetically separable	2017	115[a]
NP–NC gels	—		Environmentally friendly catalyst	2018	117[a]
Pd NPs@GC	2–4		Good immobilization capacity of Pd NPs	2019	63[a]
Pd NPs/MNP-embedded alginate particles	—		At least 10 consecutive catalytic reactions	2019	121[a]
PEI–Pd	—		Easily separated	2020	118[a]
Pd-immobilized on PEGDA-based hydrogel	2–4		Enhanced stability	2020	119[a]
CH–PdNPs	—		High stability and easy recyclability	2020	122[a]
rGO–BP–Pd	5–10		Enhanced catalytic performance	2020	120[a]
Ni–N@C	—		Favorable catalytic activity for 5 reaction cycles	2021	123
PPy/Pd hydrogel	—	Adsorption of rhodamine B	Good TOF rate constant	2017	116[a]
Pd_TMV_PEG	2–3	Reduction of Cr(VI)	Robust, and scalable synthesis	2013	124
Pd–TMV nano-biocomplexes	1–2		Retaining catalytic activity for at least 3 days	2019	126
Pd–GHJ	10	Reduction of nitroarenes	Use of ammonia borane as a hydrogen storage material for the first time	2017	125
MarGO–Pd	30	Reduction of 4-NP, CR, MB	Suitable for several biochemical applications	2020	127
Pd NPs@CNCC–AHB	9	Reduction of MB	Suitable catalyst for C–C coupling along with MB reduction	2020	128

[a] Discussed in the review.

the particle size of the palladium nanoparticles was the smallest.

In 2021, An and co-workers fabricated N-doped mesoporous carbon modified by highly dispersion nickel NPs (Ni–N@C) through the pyrolysis of Ni^{2+}/histidine cross-linked alginate hydrogels.[123] Next, the obtained Ni–N@C nano-catalyst was treated using a solution of palladium(II). Small amounts of the deposited palladium nanoparticles were found on the surface of nickel by the reduction of nickel to obtain a higher distribution of the valuable metal material (Fig. 9). The catalyst presented a good performance, where the pollutants were completely degraded in the presence of highly concentration 4-NP within a very short time. It was shown that the pre-embedded nickel nanoparticles could not only enhance the activity of palladium nanoparticles but also endow simple separation features to the catalyst. Also, this catalyst maintained favorable catalytic activity even after 5 reaction cycles.

The reports on the use of Pd-based hydrogels for environmental remediation are presented in Table 4.

4. Conclusion and future prospects

The industrial development and increasing population have resulted in an increase in the release of pollutants in the environment, threatening the health of all living organisms. These pollutants can be removed from the environment in different ways; however, it is vital to find an effective way to remove these pollutants. Catalysts are compounds that can degrade pollutants by different mechanisms, which are safe and effective for this aim. The high diversity of compounds possessing catalytic activities and possibilities of improving their catalytic yield by decreasing their size or increasing their surface area have resulted in significant progress in this field. However, although homogeneous catalysts have various advantages, including high selectivity and reactivity, they are not generally commercialized owing their difficult separation, leading to fouling and corrosion. To create heterogeneous catalysts, homogeneous catalysts can be loaded on different supports, among which hydrogels are suitable owing to their numerous advantages including high thermal stability, high mechanical strength, easy modification, and high surface area.

By applying catalytic reduction or degradation reactions, different organic pollutants such as including nitro compounds, organic dyes, hexavalent chromium, and medicinal compounds can be removed. As stated above, copper and palladium-based hydrogels can be used as an effective catalyst to remove these contaminants. Copper and palladium with fascinating features such as antibacterial, antifungal, and antimicrobial activities can be used for environmental remediation. Herein, we summarized the recent progress on the use of copper- and palladium-based hydrogels for environmental remediation. Despite the many studies on copper- and palladium-based hydrogels, there are still some challenges for their future application. In the future, hydrogel-based carriers

can be an excellent candidate for the successful administration of drugs at the desired rate and site in the body. With the creation of new hydrogels with various structural properties and hydrophobicity/hydrophilicity ratios, specific release rates and dissolution profiles may be achieved. Accordingly, these methods can be used to treat pathological illnesses such as diabetes and even cancer and enhance the delivery of more sensitive molecules. More advancements are anticipated, specifically, in the delivery of therapeutic proteins and peptides *via* hydrogels.

- Despite the progress in environmental remediation, some compounds have to be still eliminated from the environment.
- Use of different natural-based polymers such as lignin, chitin, chitosan, gum, cellulose, starch, and gelatin as supports.
- Use of low-cost approaches for the scalable production of catalysts.
- Manufacture of industrial-scale copper- and palladium-based hydrogels can be useful to eliminate environmental pollutants.
- Magnetic copper- and palladium-based hydrogels can be upgraded to exhibit high recyclability and catalytic activity to remove environmental pollutants.

Abbreviations

MNPs	Metal nanoparticles
4-NP	4-Nitrophenol
PNP	*para*-Nitrophenol
Cu	Copper
Pd NPs	Palladium nanoparticles
AN	Acrylonitrile
AAc	Acrylic acid
MA	Methacrylic acid
CTAB	Hexadecyl trimethyl ammonium bromide
4-AP	4-Aminophenol
(P(AMPS))	P(2-acrylamido-2-methyl-1-propansulfonic acid)
P(VPA)	P(vinyl phosphonic acid)
P(EGDA)	Polyethylene glycol diacrylate
(Poly(AAc–SSS–GO))	Poly(acrylic acid–sodium-sulfonate-styrene graphene oxide)
(P(AAc-*co*-AAm))	Poly(acrylic acid-*co*-acrylamide)
Cu_2O/Cu/rGO@CN	Cu_2O/Cu/reduced graphene oxide@carbon nanomaterial
MB	Methylene blue
CS	Chitosan
CMM	Cellulose microfiber mat
CB	Cresyl blue dye
CS/F	chitosan/fluorescein
CH–PAmCu–NPs	Cu NPs and ammonium persulphate
Cu@GLA–PEI–CA	Calcium alginate, polyethylene imine, and glutaraldehyde
GL	Gelatin
CR	Congo red
MO	Methyl orange
g-C_3N_4	Carbon nitride
Alg	Sodium alginate
Alg–CNBs	Alginate carbon nitride beads
N–C/Cu/N–C	N-doped porous carbon
PDA	Polydopamine
CNF	Cellulose nanofiber
rGH	Reduced graphene hydrogel
CNT	Carbon nanotube
GH	Graphene hydrogel
GO	Graphene oxide
Pd/MoS_2-rGO	Molybdenum disulfide and supported by Pd
rGSs/Fe_3O_4–Pd	Reduced graphene oxide nanosheets/magnetite-palladium
NPs	Nanoparticles
α-Fe_2O_3	Hematite
PPy	Polypyrrole
NC gels	Nanocomposite hydrogels
CNSs	Clay (synthetic hectorite) nanosheets
PVP	Polyvinylpyrrolidone
PEGDA	Polyethylene glycol diacrylate
rGO–BP–Pd	Pd-immobilized rGO and black phosphorus nanosheets
BPNS	Black phosphorus nanosheets
GC	Guanidinium-cellulose
LDHs	Layered double hydrotalcites
CS–Pd NPs	Chitosan hydrogel catalyst doped palladium nanoparticles
Ni–N@C NPs	Carbon modified by highly dispersion nickel nanoparticles

Conflicts of interest

There are no conflicts to declare.

Acknowledgements

Here, the partial support of the Research Council of Islamic Azad University, Qom Branch are acknowledged.

References

1 F. Han, V. S. R. Kambala, M. Srinivasan, D. Rajarathnam and R. Naidu, *Appl. Catal., A*, 2009, **359**, 25–40.
2 J. A. Tkaczyk, K. Mitrowska and A. Posyniak, *Sci. Total Environ.*, 2020, **717**, 137222.
3 O. P. Zhao, X. Feng, D. Huang, G. Yang and D. Astruc, *Coord. Chem. Rev.*, 2015, **287**, 114–136.
4 M. Zhang, X. Su, L. Ma, A. Khan, L. Wang, J. Wang, A. Maloletnev and C. Yang, *J. Hazard. Mater.*, 2021, **403**, 123870.
5 M. A. Zakaria, A. Menazea, A. M. Mostafa and E. A. Al-Ashkar, *Surf. Interfaces*, 2020, **19**, 100438.
6 S. Xia, L. Zhang, G. Pan, P. Qian and Z. Ni, *Phys. Chem. Chem. Phys.*, 2015, **17**, 5345–5351.
7 V. C. Lops, A. Ancona, K. Di Cesare, B. Dumontel, N. Garino, G. Canavese, S. Hérnandez and V. Cauda, *Appl. Catal., B*, 2019, **243**, 629–640.

8 V. A. Sakkas, M. A. Islam, C. Stalikas and T. A. Albanis, *J. Hazard. Mater.*, 2010, **175**, 33–44.
9 D. Ayodhya and G. Veerabhadram, *Mater. Today Energy*, 2018, **9**, 83–113.
10 S. Nataraj, K. Hosamani and T. Aminabhavi, *Desalination*, 2009, **249**, 12–17.
11 B. Shi, G. Li, D. Wang, C. Feng and H. Tang, *J. Hazard. Mater.*, 2007, **143**, 567–574.
12 J. Ma, X. Tang, Y. He, Y. Fan and J. Chen, *Desalination*, 2020, **480**, 114328.
13 I. C. da Costa Soares, Á. R. L. da Silva, E. C. M. de Moura Santos, E. V. dos Santos, D. R. da Silva and C. A. Martínez-Huitle, *J. Solid State Electrochem.*, 2020, **24**, 3245–3256.
14 K. B. Tan, M. Vakili, B. A. Horri, P. E. Poh, A. Z. Abdullah and B. Salamatinia, *Sep. Purif. Technol.*, 2015, **150**, 229–242.
15 G. Liu, M. R. Abukhadra, A. M. El-Sherbeeny, A. M. Mostafa and M. A. Elmeligy, *J. Environ. Manage.*, 2020, **254**, 109799.
16 M. Wawrzkiewicz, M. Wiśniewska, A. Wołowicz, V. M. Gun'ko and V. I. Zarko, *Microporous Mesoporous Mater.*, 2017, **250**, 128–147.
17 G. Liao, Y. Gong, L. Zhong, J. Fang, L. Zhang, Z. Xu, H. Gao and B. Fan, *Nano Res.*, 2019, **12**, 2407–2436.
18 G. Liao, J. Fang, Q. Li, S. Li, Z. Xu and B. Fang, *Nanoscale*, 2019, **11**, 7062–7096.
19 G. Liao, J. Chen, W. Zeng, C. Yu, C. Yi and Z. Xu, *J. Phys. Chem. C*, 2016, **45**, 25935–25944.
20 G. Liao, Q. Li, W. Zhao, Q. Pang, H. Gao and Z. Xu, *Appl. Catal., A*, 2018, **549**, 102–111.
21 G. Liao, W. Zhao, Q. Li, Q. Pang and Z. Xu, *Chem. Lett.*, 2017, **46**, 1631–1634.
22 Q. Wu, J. Wang, Z. Wang, Y. Xu, Z. Xing, X. Zhang, Y. Guan, G. Liao and X. Li, *J. Mater. Chem. A*, 2020, **8**, 13685–13693.
23 H. Zhu, S. Cai, G. Liao, Z. F. Gao, X. Min, Y. Huang, S. Jin and X. Fan, *ACS Catal.*, 2021, **11**(24), 14751–14771.
24 R. Sankar, P. Manikandan, V. Malarvizhi, T. Fathima, K. S. Shivashangari and V. Ravikumar, *Spectrochim. Acta, Part A*, 2014, **121**, 746–750.
25 M. M. Khin, A. S. Nair, V. J. Babu, R. Murugan and S. Ramakrishna, *Energy Environ. Sci.*, 2012, **5**, 8075–8109.
26 W.-J. Liu, T.-T. Qian and H. Jiang, *Chem. Eng. J.*, 2014, **236**, 448–463.
27 M. D. Argyle and C. H. Bartholomew, *Catalysts*, 2015, **5**, 145–269.
28 M. Nasrollahzadeh, M. Sajjadi, J. Dadashi and H. Ghafuri, *Adv. Colloid Interface Sci.*, 2020, **276**, 102103.
29 M. Chen, P. Liu, C. Wang, W. Ren and G. Diao, *New J. Chem.*, 2014, **38**, 4566–4573.
30 K. M. Lee, C. W. Lai, K. S. Ngai and J. C. Juan, *Water Res.*, 2016, **88**, 428–448.
31 J. K. H. Wong, H. K. Tan, S. Y. Lau, P.-S. Yap and M. K. Danquah, *J. Environ. Chem. Eng.*, 2019, **7**, 103261.
32 R. K. Ibrahim, M. Hayyan, M. A. AlSaadi, A. Hayyan and S. Ibrahim, *Environ. Sci. Pollut. Res.*, 2016, **23**, 13754–13788.
33 N. Y. Nadaf and S. S. Kanase, *Arabian J. Chem.*, 2019, **12**, 4806–4814.
34 H. Dabhane, S. Chatur, G. Jadhav, P. Tambade and V. Medhane, *Environ. Chem. Ecotoxicol.*, 2021, **3**, 160–171.
35 A. J. Kora and L. Rastogi, *Arabian J. Chem.*, 2018, **11**, 1097–1106.
36 Z. Gong, T. Ma and F. Liang, *J. Alloys Compd.*, 2021, **873**, 159802.
37 S. Joseph and B. Mathew, *J. Mol. Liq.*, 2015, **204**, 184–191.
38 N. A. Peppas, J. Z. Hilt, A. Khademhosseini and R. Langer, *Adv. Mater.*, 2006, **18**, 1345–1360.
39 S. Wang, T. Vincent, C. Faur and E. Guibal, *Appl. Sci.*, 2018, **8**, 264–281.
40 B. V. Slaughter, S. S. Khurshid, O. Z. Fisher, A. Khademhosseini and N. A. Peppas, *Adv. Mater.*, 2009, **21**, 3307–3329.
41 G.-J. Jiao, J. Ma, Y. Li, D. Jin, J. Zhou and R. Sun, *J. Hazard. Mater.*, 2022, **421**, 126722.
42 Q. Luo, H. Yuan, M. Zhang, P. Jiang, M. Liu, D. Xu, X. Guo and Y. Wu, *J. Hazard. Mater.*, 2021, **401**, 123432.
43 D. Dou, D. Wei, X. Guan, Z. Liang, L. Lan, X. Lan, P. Liu, H. Mo and P. Lan, *J. Hazard. Mater.*, 2022, **423**, 127137.
44 Y. Meng, J. Yin, T. Jiao, J. Bai, L. Zhang, J. Su, S. Liu, Z. Bai, M. Cao and Q. Peng, *J. Mol. Liq.*, 2020, **298**, 112010.
45 M. Liao, H. Qin, W. Guo, P. Gao and H. Xiao, *Ceram. Int.*, 2021, **47**, 33667–33677.
46 Y. Zhang, S. Liu, T. Li, L. Zhang, U. Azhar, J. Ma, C. Zhai, C. Zong and S. Zhang, *Carbohydr. Polym.*, 2020, **236**, 116021.
47 A. L. Mohamed, A. A. Soliman, E. A. Ali, N. Y. Abou-Zeid and A. A. Nada, *Int. J. Biol. Macromol.*, 2020, **163**, 888–897.
48 J. F. Souza, G. P. Costa, R. Luque, D. Alves and A. R. Fajardo, *Catal. Sci. Technol.*, 2019, **9**, 136–145.
49 H. Ozay, P. Ilgin and O. Ozay, *Int. J. Hydrogen Energy*, 2020, **45**, 17613–17624.
50 D. George, P. U. Maheswari and K. M. S. Begum, *Int. J. Biol. Macromol.*, 2019, **132**, 784–794.
51 S. K. H Gulrez, S. Al-Assaf and G. O Phillips, *Prog. Mol. Environ. Bioeng.: Anal. Model. Technol. Appl.*, 2011, **117150**, 117–150.
52 E. M. Ahmed, *J. Adv. Res.*, 2015, **6**, 105–121.
53 D. Zhou, L. Zhang and S. Guo, *Water Res.*, 2005, **39**, 3755–3762.
54 B. Benguella and H. Benaissa, *Water Res.*, 2002, **36**, 2463–2474.
55 S. Wunder, F. Polzer, Y. Lu, Y. Mei and M. Ballauff, *J. Phys. Chem. C*, 2010, **114**, 8814–8820.
56 P. Herves, M. Perez-Lorenzo, L. M. Liz-Marzan, J. Dzubiella, Y. Lu and M. Ballauff, *Chem. Soc. Rev.*, 2012, **41**, 5577–5587.
57 A. Zinchenko, Y. Miwa, L. I. Lopatina, V. G. Sergeyev and S. Murata, *ACS Appl. Mater. Interfaces*, 2014, **6**, 3226–3232.
58 A. Lim Teik Zheng, T. Phromsatit, S. Boonyuen and Y. Andou, *FlatChem*, 2020, **23**, 100174.
59 K. Akhtar, S. B. Khan, E. M. Bakhsh, T. Kamal, S. Ahmad, A. M. Asiri and Y. Anwar, *Int. J. Biol. Macromol.*, 2022, **208**, 56–69.
60 L. Ge, M. Zhang, R. Wang, N. Li, L. Zhang, S. Liu and T. Jiao, *RSC Adv.*, 2020, **10**, 15091–15097.
61 T. Kamal, S. B. Khan and A. M. Asiri, *Environ. Pollut.*, 2016, **218**, 625–633.

62 A. Khalil, N. Ali, A. Khan, A. M. Asiri and T. Kamal, *Int. J. Biol. Macromol.*, 2020, **164**, 2922–2930.
63 X. Li, F. Dong, L. Zhang, Q. Xu, X. Zhu, S. Liang, L. Hu and H. Xie, *Chem. Eng. J.*, 2019, **372**, 516–525.
64 J. Li, C.-y. Liu and Y. Liu, *J. Mater. Chem.*, 2012, **22**, 8426–8430.
65 N. Sahiner, H. Ozay, O. Ozay and N. Aktas, *Appl. Catal., A*, 2010, **385**, 201–207.
66 N. Jabeen, Z. H. Farooqi, A. Shah, A. Ali, M. Khurram, K. Mahmood, N. Sahiner and M. Ajmal, *J. Porous Mater.*, 2021, **28**, 1563–1576.
67 J. Dhiman, S. O. Prasher, E. ElSayed, R. M. Patel, C. Nzediegwu and A. Mawof, *J. Cleaner Prod.*, 2021, **311**, 127644.
68 D. Berillo and A. Cundy, *Carbohydr. Polym.*, 2018, **192**, 166–175.
69 N. Alhokbany, T. Ahama, Ruksana, M. Naushad and S. M. Alshehri, *Composites, Part B*, 2019, **173**, 106950.
70 Z. Khorsandi, A. R. Hajipour, M. R. Sarfjoo and R. S. Varma, *Green Chem.*, 2021, **23**, 5222–5229.
71 H.-C. Li, W.-J. Liu, H.-X. Han and H.-Q. Yu, *J. Mater. Chem. A*, 2016, **4**, 11680–11687.
72 N. Ali, T. Kamal, M. Ul-Islam, A. Khan, S. J. Shah and A. Zada, *Int. J. Biol. Macromol.*, 2018, **111**, 832–838.
73 M. Mifsud, K. V. Parkhomenko, I. W. Arends and R. A. Sheldon, *Tetrahedron*, 2010, **66**, 1040–1044.
74 J. Zhong, Q. Wang, J. Zhou, D. Chen and Z. Ji, *Appl. Surf. Sci.*, 2016, **367**, 342–346.
75 C. Zhou, J. Bai, Y. Zhang, J. Li, Z. Li, P. Jiang, F. Fang, M. Zhou, X. Mei and B. Zhou, *J. Hazard. Mater.*, 2021, **401**, 123232.
76 M. Noman, M. Shahid, T. Ahmed, M. B. K. Niazi, S. Hussain, F. Song and I. Manzoor, *Environ. Pollut.*, 2020, **257**, 113514.
77 M. I. Din, R. Khalid, Z. Hussain, T. Hussain, A. Mujahid, J. Najeeb and F. Izhar, *Crit. Rev. Anal. Chem.*, 2020, **50**, 322–338.
78 R. Kottappara, S. C. Pillai and B. K. Vijayan, *Inorg. Chem. Commun.*, 2020, **121**, 108181.
79 A. J. Kora and L. Rastogi, *Ind. Crops Prod.*, 2016, **81**, 1–10.
80 N. Sahiner, S. Butun and P. Ilgin, *Colloids Surf., A*, 2011, **386**, 16–24.
81 N. Sahiner and O. Ozay, *Curr. Nanosci.*, 2012, **8**, 367–374.
82 N. Sahiner and S. Sagbas, *Colloids Surf., A*, 2013, **418**, 76–83.
83 J. Paul Guin, Y. K. Bhardwaj and L. Varshney, *J. Appl. Polym. Sci.*, 2018, **135**, 46200–46212.
84 F. Naseer, M. Ajmal, F. Bibi, Z. H. Farooqi and M. Siddiq, *Polym. Compos.*, 2018, **39**, 3187–3198.
85 R. Su, S. Ge, H. Li, Y. Su, Q. Li, W. Zhou, B. Gao and Q. Yue, *Sci. Total Environ.*, 2019, **693**, 133657.
86 Y. Y. Li Sip, D. W. Fox, L. R. Shultz, M. Davy, H.-S. Chung, D.-X. Antony, Y. Jung, T. Jurca and L. Zhai, *ACS Appl. Nano Mater.*, 2021, **4**, 6045–6056.
87 S. Haider, T. Kamal, S. B. Khan, M. Omer, A. Haider, F. U. Khan and A. M. Asiri, *Appl. Surf. Sci.*, 2016, **387**, 1154–1161.
88 C. Saldías, D. D. Díaz, S. Bonardd, C. Soto-Marfull, A. Cordoba, S. Saldías, C. Quezada, D. Radic and Á. Leiva, *Carbohydr. Polym.*, 2018, **180**, 200–208.
89 S. Sharma, Deepak, A. Kumar, S. Afgan and R. Kumar, *ChemistrySelect*, 2017, **2**, 11281–11287.
90 S. Wang, Z. Xiao, X. Ma, Z. Zhao, D. Guo, Y. Chen, S. Zhai, Q. An and D. Yang, *Appl. Catal., A*, 2018, **568**, 105–113.
91 S. Ahmad, S. B. Khan, A. M. Asiri, H. M. Marwani and T. Kamal, *J. Sol-Gel Sci. Technol.*, 2020, **96**, 382–394.
92 S. B. Khan, S. Ahmad, T. Kamal, A. M. Asiri and E. M. Bakhsh, *Int. J. Biol. Macromol.*, 2020, **164**, 1087–1098.
93 Z. Zhao, Z. Xiao, C. Qin, H. Lv, L. Qin, W. Niu, S. Zhai and Q. An, *Ind. Crops Prod.*, 2021, **164**, 113413.
94 A. L. T. Zheng, S. Sabidi, T. Ohno, T. Maeda and Y. Andou, *Chemosphere*, 2022, **286**, 131731.
95 M. Ajmal, S. Demirci, M. Siddiq, N. Aktas and N. Sahiner, *New J. Chem.*, 2016, **40**, 1485–1496.
96 Y. Sun, F. Zhang, L. Xu, Z. Yin and X. Song, *J. Mater. Chem. A*, 2014, **2**, 18583–18592.
97 L. V. Lombardo Lupano, J. M. Lázaro Martínez, L. L. Piehl, E. Rubín de Celis, R. M. Torres Sánchez and V. Campo Dall' Orto, *Langmuir*, 2014, **30**, 2903–2913.
98 N. Sahiner, F. Seven and H. Al-lohedan, *Water, Air, Soil Pollut.*, 2015, **226**, 122–133.
99 S. Demirci and N. Sahiner, *Water, Air, Soil Pollut.*, 2015, **226**, 64–76.
100 A. Zinchenko, Y. Che, S. Taniguchi, L. I. Lopatina, V. G. Sergeyev and S. Murata, *J. Nanopart. Res.*, 2016, **18**, 179–187.
101 J. Liu, D. Su, J. Yao, Y. Huang, Z. Shao and X. Chen, *J. Mater. Chem. A*, 2017, **5**, 4163–4171.
102 J. Ding, Q. Li, L. Zhao, X. Li, Q. Yue and B. Gao, *RSC Adv.*, 2017, **7**, 17599–17611.
103 R. Su, Q. Li, R. Huang, L. Zhao, Q. Yue, B. Gao and Y. Chen, *J. Taiwan Inst. Chem. Eng.*, 2018, **91**, 235–242.
104 J. Ding, Q. Li, X. Xu, X. Zhang, Y. Su, Q. Yue and B. Gao, *Carbohydr. Polym.*, 2018, **190**, 12–22.
105 R. Su, F. Wang, J. Ding, Q. Li, W. Zhou, Y. Liu, B. Gao and Q. Yue, *Carbohydr. Polym.*, 2019, **220**, 202–210.
106 T. Kamal, *Polym. Test.*, 2019, **77**, 105896–105903.
107 A. Upadhyay, A. Narula and C. P. Rao, *ACS Appl. Bio Mater.*, 2020, **3**, 8619–8626.
108 L. Qin, R. Ru, J. Mao, Q. Meng, Z. Fan, X. Li and G. Zhang, *Appl. Catal., B*, 2020, **269**, 118754.
109 P. Xu, C. Cen, M. Zheng, Y. Wang, Z. Wu and Z. Teng, *Mater. Chem. Phys.*, 2020, **253**, 123444.
110 A. Intanin, P. Inpota, T. Chutimasakul, J. Tantirungrotechai, P. Wilairat and R. Chantiwas, *Molecules*, 2020, **25**, 1798.
111 Y. Chen, R. Su, F. Wang, W. Zhou, B. Gao, Q. Yue and Q. Li, *Chemosphere*, 2021, **270**, 129295.
112 W. Peng, Y. Yan, D. Zhang, Y. Zhou, D. Na, C. Xiao, C. Yang, G. Wen and J. Zhang, *Colloids Surf., A*, 2021, **624**, 126809.
113 Z. Zhang, T. Sun, C. Chen, F. Xiao, Z. Gong and S. Wang, *ACS Appl. Mater. Interfaces*, 2014, **6**, 21035–21040.
114 J. Ji, Y. Li, W. Fu, Z. Cui, J. Shen and M. Ye, *J. Colloid Interface Sci.*, 2017, **505**, 983–994.

115 Y. Feng, H. Zhang, B. Xin and J. Wu, *J. Colloid Interface Sci.*, 2017, **506**, 154–161.
116 T. Yao, W. Jia, X. Tong, Y. Feng, Y. Qi, X. Zhang and J. Wu, *J. Colloid Interface Sci.*, 2018, **527**, 214–221.
117 D. Varade and K. Haraguchi, *eXPRESS Polym. Lett.*, 2018, **12**, 996–1004.
118 Y. Feng, J. Yin, S. Liu, Y. Wang, B. Li and T. Jiao, *ACS Omega*, 2020, **5**, 3725–3733.
119 K.-K. Kang, K. Shim and C.-S. Lee, *Colloids Surf., A*, 2020, **593**, 124607.
120 R. Wang, M. Zhang, B. Ge, L. Zhang, J. Zhou, S. Liu and T. Jiao, *J. Mol. Liq.*, 2020, **310**, 113083.
121 M. Xia, S.-M. Kang, G.-W. Lee, Y. S. Huh and B. J. Park, *J. Ind. Eng. Chem.*, 2019, **73**, 306–315.
122 J. Zhu, X. Zhang, Z. Qin, L. Zhang, Y. Ye, M. Cao, L. Gao and T. Jiao, *Colloids Surf., A*, 2021, **611**, 125889.
123 H. Liu, Y.-n. Qin, H.-y. Li, L.-x. Gai, Q.-d. An, S.-r. Zhai, Z.-y. Xiao and L. Cui, *Int. J. Biol. Macromol.*, 2021, **173**, 160–167.
124 C. Yang, C.-H. Choi, C.-S. Lee and H. Yi, *ACS Nano*, 2013, **7**, 5032–5044.
125 P. Eghbali, B. Nişancı and Ö. Metin, *Pure Appl. Chem.*, 2018, **90**, 327–335.
126 I. Sadeghi, E. Y. Liu, H. Yi and A. Asatekin, *ACS Appl. Nano Mater.*, 2019, **2**, 5233–5244.
127 L. Minati, G. Speranza, V. Micheli, M. Dalla Serra and M. Clamer, *Dalton Trans.*, 2020, **49**, 3333–3340.
128 B. Wang, M. Ran, G. Fang, T. Wu, Q. Tian, L. Zheng, L. Romero-Zerón and Y. Ni, *Cellulose*, 2020, **27**, 6995–7008.